Industrial Crops & Products 159 (2021) 113027

Contents lists available at ScienceDirect

Industrial Crops & Products

journal homepage: www.elsevier.com/locate/indcrop

Future trends for the analysis of guayulins in guayule (*Parthenium argentatum* Gray) resins

Juana Rozalén [a], M. Mercedes García [a], Amaya Zalacain [a], Horacio López-Córcoles [b], Jorge Hurtado de Mendoza [c], Katrina Cornish [d], Manuel Carmona [e,f,*]

[a] Universidad de Castilla-La Mancha, Catedra de Química Agrícola, Escuela Técnica Superior de Ingenieros Agrónomos y de Montes, Campus Universitario s/n, 02071, Albacete, Spain
[b] Instituto Técnico Agronómico Provincial, ITAP, Parque empresarial Campollano, 2ª Avenida, 61, 02007, Albacete, Spain
[c] Grilab, Americo Castro 94, 28050, Madrid, Spain
[d] The Ohio State University, College of Food, Agricultural and Environmental Sciences, Wooster, OH, 44691, USA
[e] Universidad de Castilla-La Mancha, Institute for Regional Development (IDR), Food Quality Research Group, Campus Universitario s/n, Albacete, 02071, Spain
[f] Universidad Europea de Madrid, School of Architecture, Engineering and Design, Food Technology Lab, C/ Tajo s/n, 28670, Villaviciosa de Odón (Madrid), Spain

ARTICLE INFO

Keywords:
Guayule
Resins
Guayulins
LC–MS
ESI-MS
MALDI-TOF

ABSTRACT

Guayule (*Parthenium argentatum* Gray) is a promising alternative and renewable source of natural rubber/latex. There is a general acceptance that to successfully industrialize the cultivation of guayule, it will be necessary to valorize all of its co-products, including resins, which can reach 16 % of weight of dry matter. Guayule resins have been reported to have antifungal, insect antifeedant and wood protector activities, although it remains to be clearly established which compounds are responsible for such actions. Here, we focus on a terpene family present in guayule resin that is a candidate for these activities, the sesquiterpenes, which are present in significant amounts (10–15 %). We studies the versatility of the most common analytical method used in their analysis, HPLC-UV, with mass spectrometry techniques including LC–MS, ESI-TOF and MALDI-TOF to address the following objectives: 1) to explore whether there are other members of the guayulins family, 2) to determine the applicability of new methods based on mass spectrometry, and 3) to establish the relationship between the four known major guayulins in the seasonal changes described by other authors. Our results have allowed us to: tentatively identify a new member of this family and to suggest the existence of others; propose changes to the chromatographic approaches currently used; extend the use of mass spectrometry (direct identification and monitoring of purification of guayulins); and finally, demonstrate that the content of guayulins A and B decreases at the start of winter when the most active period of natural rubber biosynthesis begins.

1. Introduction

Guayule (*Parthenium argentatum* Gray) is a silver-gray perennial shrub native to the semi-arid areas of northern Mexico that has been previously used as a source of natural rubber (Coffelt et al., 2015). Recent years have witnessed a renewed interest in guayule because, as opposed to the traditional source of natural rubber, the rubber tree (*Hevea brasiliensis*), the latex obtained from guayule is hypoallergenic (Cornish et al., 2009).

Guayule offers several other notable advantages over *H. brasiliensis*. As it requires relatively little water and is very resistant to pests, it can be grown in an environmentally responsible manner without the need for pesticides (Foster and Coffelt, 2005). Also, unlike *H. brasiliensis,* it can be grown far from the tropical zone, and in areas close to the centers of utilization of the raw material, reducing the environmental impact of transport (Soratana et al., 2017). This latter benefit has led to the investigation of guayule as a sustainable agricultural crop in semi-desert areas (including Spain and France) that are being developed to combat climate change (Snoeck et al., 2015). Despite all these advantages the commercialization of guayule rubber has been slow because of its higher price relative to *H. brasiliensis* natural rubber (a low cost commodity), and it is only currently available on a small scale for research projects and the development of prototypes. Another reason for the poor industrial commercialization of guayule is the limited level of exploitation

* Corresponding author at: Universidad de Castilla-La Mancha, Institute for Regional Development (IDR), Food Quality Research Group, Campus Universitario s/n, Albacete, 02071, Spain.
E-mail address: manuel.carmona@uclm.es (M. Carmona).

https://doi.org/10.1016/j.indcrop.2020.113027
Received 20 March 2020; Received in revised form 27 September 2020; Accepted 16 October 2020
Available online 5 November 2020

of its co-products (Sfeir et al., 2014). Chief among them is guayule resin, which can reach 8.9–16.3 % weight of dry matter (Luo and Abdel-Haleem, 2019). Indeed, guayule resin is a commercially relevant co-product, as it is present in greater quantities than the raw material (natural rubber) for which the plant is cultivated (Luo and Abdel-Haleem, 2019; Placido et al., 2020). The resin content of guayule has increased significantly through traditional breeding processes (Nakayama, 2005; Sidhu et al., 1995) that sought to increase the biomass or yield of rubber, which is usually less than 6% for almost all accessions after growing the plant for 2.5 years (Luo and Abdel-Haleem, 2019; Placido et al., 2020), although in some special cases it can approach 9% (Hunsaker et al., 2019). The concentration of natural rubber has not been improved using approaches that employ genetic modification of the expression of different metabolic pathways (Veatch et al., 2005; Dong et al., 2013; Placido et al., 2020). Likewise, no improvement in the concentration of natural rubber was seen in field trials, though in some cases there was a significant increase in resin content (Veatch et al., 2005). Moreover, the use of irrigation showed that it is easier to increase the concentration and yield of resin per hectare than the yield of natural rubber, which increases due to the higher production of biomass that compensates for reductions in the concentration of natural rubber (Hunsaker and Elshikha, 2017). Thus, more attention should be paid to the exploitation of the resin to support the commercialization of guayule and its coproducts. Indeed, the commercialization of guayule resin would undoubtedly give a major boost to the use of this crop for a range of applications suggested in recent years, including as an asphalt binder (Lusher and Richardson, 2015), in sustainable flexible pavement (Hemida and Abdelrahman, 2020), biocomposite boards (Bajwa et al., 2017), and adhesives or strippable coatings (Nakayama, 2005). Moreover, guayule resin has been proposed as a plant-based material for the microencapsulation of bioactive volatiles for non-food purposes (Pascual Villalobos and López, 2013), and as an acaricide in the agro-food or veterinary industry (Jara et al., 2019). There are also potential applications that exploit its bioactivity as an antifungal or anti-termite agent and as a wood protector (Bultman et al., 1991; Maatooq et al., 1996; Nakayama et al., 2001; Nakayama, 2005; Holt et al., 2012). Indeed, these applications could have a greater added value than those previously mentioned, although it remains unclear which compounds are responsible for these effects.

Triterpenes (including argentatins), sterols and fatty acids, and sesquiterpene and sesquiterpene esters (including guayulins) are the most relevant compounds in guayule resin (Cheng et al., 2020). Compounds belonging to the guayulin family have been found only in guayule and in some hybrids (Teetor et al., 2009). Guayulins are both isoprenoids and aromatic acid esters (Teetor et al., 2009): guayulins A and B are the *trans*-cinnamic and *p*-anisic acid esters, respectively, of partheniol, a sesquiterpene alcohol; and guayulin C and D are likely formed by the oxidation of guayulin A and B, respectively (Schloman et al., 1983; Martínez et al., 1986) (Fig. 1). In addition to the aforementioned guayulins, some authors suggest the possibility of other members of this family (Teetor et al., 2009). Guayulin content varies greatly depending on the time of year (Schloman et al., 1986) and on the part of the plant analyzed (Spano et al., 2018). Traditionally, attention has focused on guayulins A and B (Schloman et al., 1986; Coffelt et al. (2009), although high levels of guayulin C have been found recently, especially in leaves (Spano et al., 2018). It remains to be established, however, whether this high content is due to its natural presence or whether it has formed later by oxidation of guayulin A, as suggested by some studies (Schloman et al., 1983; Martinez et al., 1986; Spano et al., 2018).

Any future use of guayulins as by-products of guayule cultivation will be contingent upon resin separation and purification cost and efficiency (Cheng et al., 2020), and also on the development of reliable, accurate and sensitive analytical methods for their identification and quantification, which generally require much effort and, above all, time (Taurines et al., 2019). Presently, analytical methods are considered cost-inefficient, which limits the number of samples that can be processed (Abdel-Haleem et al., 2019). For example, the pre-extraction grinding processes may lead to sample heating (Pearson et al., 2013), and frequent breaks may be required before achieving the particle size generally recommended for analytical determination ($\leq$0.5 mm) (Suchat et al., 2013). Once extracted – usually from the stem – guayulins are typically quantified by high performance liquid chromatography and identified by UV detection (HPLC-UV; range 255–278 nm). Table 1 briefly summarizes the characteristics of the commonly used HPLC methods for the analysis of guayulins.

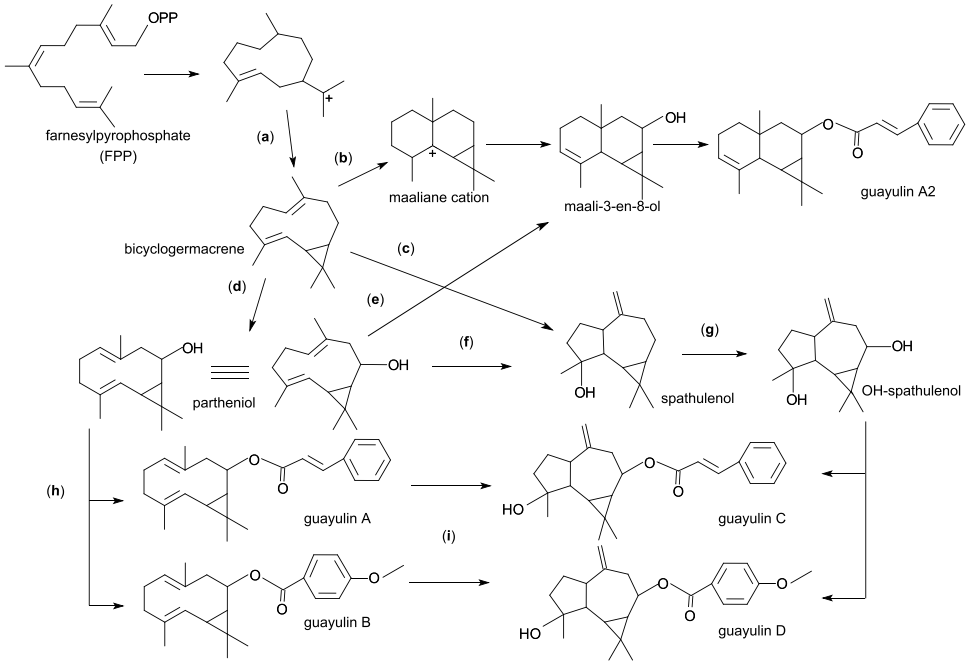

Fig. 1. Possible biosynthetic routes of guayulins. Elaborated from our own results and those Durán-Peña et al., 2015 (a), Gijsen et al., 1995 (b), Chaves et al., 2003 (c), Walter, 1944 (d, h), Maatooq, 2002 (e), Asakawa and Noma, 2010 (e), Tran and Cramer, 2014 (f), Crevoisier et al., 1984 (g) and Schloman et al., 1983 (h,i).

Table 1
Key features of selected literature using reverse-phase HPLC methods of analysis for guayulins in extracts from guayule.

Reference	(Spano et al., 2018)	(Teetor et al., 2009; Cornish et al., 2009; Coffelt et al., 2009; Ray et al., 2007)	(Sidhu et al., 1995)	(Martínez et al., 1986)	(Schloman et al., 1983)	(Behl et al., 1983)	(Proksch et al., 1981)
Stationary phase (mm × mm × μm)	Ascentis® C18 (250 × 4.6 × 5)	Microsorb-MV (250 × 4.6 × 5)	RP-C18 column (300 × 3.9 ×[a])	C18 column	MicroPak MCH-10 (300 × 4.6 × 10)	Altex Ultrasphere ODS type (150 × 4.6 × 5)	Lichrosorb RP-18 (250 × 4.6 × 10)
Mobile phase (B), (A is always water)	CH_3CN	CH_3CN	MeOH	MeOH	CH_3CN	MeOH	CH_3CN
Gradient/ Isocratic	20:80	20:80 to 00:100	11:89	[a]	50:50 to 25:75	07:93	25:75
Flow Rate (mL min^{-1})	1.5	1.5	1	[a]	[a]	1	2.5
Run time (min)	25	36	[a]	[a]	[a]	9	10

[a] Information not available in the paper.

HPLC-UV is considered the reference and gold standard method for the determination of guayulins, and its versatility has been investigated in detail in the present study. We have also examined other available analytical methods to characterize guayulin content, including techniques that can also be used to monitor these and other compounds of interest in the plant or during their extraction and subsequent isolation. In particular, we have assessed the versatility of mass spectrometry (MS) analyses, now routinely available in analytical laboratories. In addition to the main aim of the work, which is to examine new methods of analysis in the determination of these compounds, we have sought to determine whether other members of this family might exist, and whether the seasonal variation proposed by some authors is responsible for the natural increase in guayulin C content during autumn-winter period.

2. Materials and methods

2.1. Plant material, sampling and processing

The guayule accessions 11619 and CAL-1 (a hybrid of *P. argentatum* and *P. tomentosum* var. *tomentosum*) were planted in May 2017 in Santa Cruz de la Zarza (Toledo, Spain). Plots consisted of 9 blocks, each of 3 m width and 8 m length, spaced 2 m apart. Every block had 9 columns and 2 rows spaced 1.5 m apart and with 20 cm between plants; 80 plants were placed in a staggered pattern per cultivar, giving a density of 33,333 plants/hectare. Beginning in 2018, 12 plants were randomly selected along the growing season (June, July, September and November 2018, and April 2019), cut 5 cm above the ground and packaged into kraft bags. To determine dry biomass, whole plants were dried at 60 °C for 48 h to achieve a moisture content of 12 %, and leaves were then manually removed from the stem.

Stems were cut into pellets of about 1 cm in length using a manual cutter, and thereafter grounded to a 0.5-mm particle size using a centrifuge grinder (Retsch centrifugal Mill ZM1, Haan, Germany). Leaves were directly grounded to a 0.5-mm particle size using the same method. Dried ground samples of stems and leaves were stored in closed screw-cap glass vessels at 4 °C until analysis.

2.2. Resin extraction

Resin extraction was performed by accelerated solvent extraction (ASE) with acetone in a Speed Extractor (model E-915; Büchi, Postfach, Switzerland). A sample of 1 ± 0.005 g of guayule was weighed and homogenized with ~32.5 g of sand as a dispersing agent to fill the stainless steel 80-mL extraction cell, leaving 1-cm free space. A cellulose acetate filter was also placed at the top and bottom of each cell to avoid sample contamination. The extraction conditions were similar to those described by Suchat et al. (2003) with slight modifications to account for the different extraction appartus: extraction temperature 40 °C, pressure 100 bar, 3 cycles, hold time 20 min, discharge 3 min.

Resins were collected in a 250-mL flask and transferred to a pre-weighed flask. Solvent evaporation was performed in a parallel Multivapor P-6 system (Büchi) at 45 °C and 500 mbar. After evaporation, the pre-weighed flasks were placed in a desiccator for 30 min before final weighing, and the resin or natural rubber percentage was determined gravimetrically. Each sample was extracted three times and the extraction yield was calculated.

2.3. High-performance liquid chromatography–diode array detection

Twenty microliters of resin dissolved in ethanol (10 mg mL^{-1}) was injected into an Agilent 1200 HPLC chromatograph (Agilent Technologies, Palo Alto, CA) equipped with a diode array detector (DAD) (Agilent G1315D), and coupled to an Agilent ChemStation (version B.03.01) data-processing station. Separation was performed at 30 °C in a reverse-phase ACE Excel 3 C18-PentaFluorPhenyl (PFP) column (150 × 4.6 mm, 3 μm particle size) protected with an ACE Excel HPLC Pre-column Filter (0.5 μm particle size) (both from Advanced Chromatography Technologies Ltd., Reading, Berkshire, UK). The solvents were water (solvent A) and acetonitrile (solvent B); the elution gradient for solvent B was as follows: 0 min, 60 %; 10 min, 60 %; 20 min, 80 % and hold 5 min; 35 min, 100 % and hold 2 min. Compounds were detected with a DAD and compared with the corresponding published UV spectra, wherein the main guayulins A and C have a maximum absorption at 276 nm and guayulin B and D at 255 nm. All analyses were performed in duplicate.

Quantification was carried out using a five levels calibration curve (2.5−250 ppm, r2 = 0.997) of guayulin A standard isolated in our lab. Low weight molecular guayule rubber (LMWGR) was removed from resin extract according to Zoeller et al., 1994. Then, resin free of LMWGR was fractionated using flash chromatography (VersaFlash Station System I equipped with a Versaflash cartridge 23 mm x 110 mm, containing Spherical C18 bonded silica 30 g, 20–45 μm) employing acetonitrile:water (80:20) as solvent, with a flow rate of 20 mL/min. Fractionation procedure was followed using HPLC-DAD. The fraction containing guayulin A was evaporated under vacuum and crystalized from hexane/chloroform as suggested by Martinez et al. (1986). Their molecular weight and mass fragmentation pattern were confirmed by LC—MS.

2.4. Liquid chromatography–mass spectrometry

A Dionex Ultimate 3000 UHPLC system coupled to a Q-exactive hybrid quadrupole-orbitrap mass spectrometer *via* an electrospray source ionization (ESI) interface (ThermoFisher Scientific, Waltham, MA) was used for resin analysis. Resins were dissolved in ethanol at a concentration of 10 mg mL^{-1}. Chromatographic separation was carried out on an ACE Excel C18-PFP column (100 × 2.1 mm, 2 μm particle size). The flow rate of the mobile phase was 500 μL min^{-1}, the injection volume was 5 μL and the initial gradient was 5% B (acetonitrile) hold 1

min, 1–7 min 95 % B, 7–9 min hold 95 %. Analyses were conducted in negative and positive ion mode, and the operating parameters were optimized as follows: capillary voltage, 3.5/-3.5 kV; drying gas temperature, 400 °C; with the nebulizer gas, curtain gas and auxiliary gas parameters set at 40, 1 and 20 arbitrary units, respectively. For full-scan MS analysis, the spectra were recorded in the 100–900 *m/z* range with a mass resolution of 70,000 and the accuracy mass below 2 ppm. The CFM-ID web server v3.0 was used to annotate the fragments obtained in MS/MS experiments.

2.5. Matrix-assisted laser desorption ionization–time-of-flight mass spectrometry

Resins were mixed with a commercial MALDI matrix (DCTB, 10 mg mL^{-1} in trihydrofuran) and silver trifluoroacetate (AgTFA, 2 mg mL^{-1} in ethanol) in the following ratio: matrix:AgTFA:sample (20:0.5:2). A Bruker Daltonik Ultraflex MALDI time-of-flight (TOF/TOF) mass spectrometer (Bremen, Germany) was used for analysis in positive reflector mode with a detection range up to 5000 Da, applying a mass deflection of 850 Da to prevent the matrix and silver salt-clusters saturating the detector.

2.6. Electrospray ionization–time-of-flight mass spectrometry

Resins were dissolved in acetone to a concentration of 2 mg mL^{-1} and a ratio of 1:200 in methanol + 0.1 % formic acid was used for analysis. The sample was introduced into a maXis II electrospray ionization TOF spectrometer (ESI–TOF) (Bruker Daltonik) using an infusion pump at a flow rate of 3 μL min^{-1}. Recordings were made in the 100–4500 Da range with accurate external mass calibration.

3. Results and discussion

3.1. Reference method: characterization of four well-known guayulins in stems and leaves

All the methods tabulated in Table 1 used high proportions (>50 %) of either acetonitrile or methanol as a mobile phase – operated in either isocratic or gradient mode – to achieve chromatographic separation of the four guayulins in about 25 min. A representative chromatogram of the resin fraction extracted from the stems of a 2-year-old adult guayule plant using the ASE technique as described in section 2.3 is shown in Fig. 2. The four major peaks correspond to guayulin compounds: the most polar compounds, guayulin D and C, and the less polar compounds, guayulin B and A, which have longer retention times.

The UV absorption spectra of guayulin D and B overlap as they have the same constituent, *p*-anisic acid, with a maximum absorption of ~256 nm (Fig. 2). The absorption spectra for guayulin C and A were different to D and B and both showed a maximum at 276–278 nm, as they share the same constituent, *trans*-cinnamic acid (Fig. 2).

The concentration of guayulins in resin varies widely, and is dependent on numerous factors including soil type, climate,

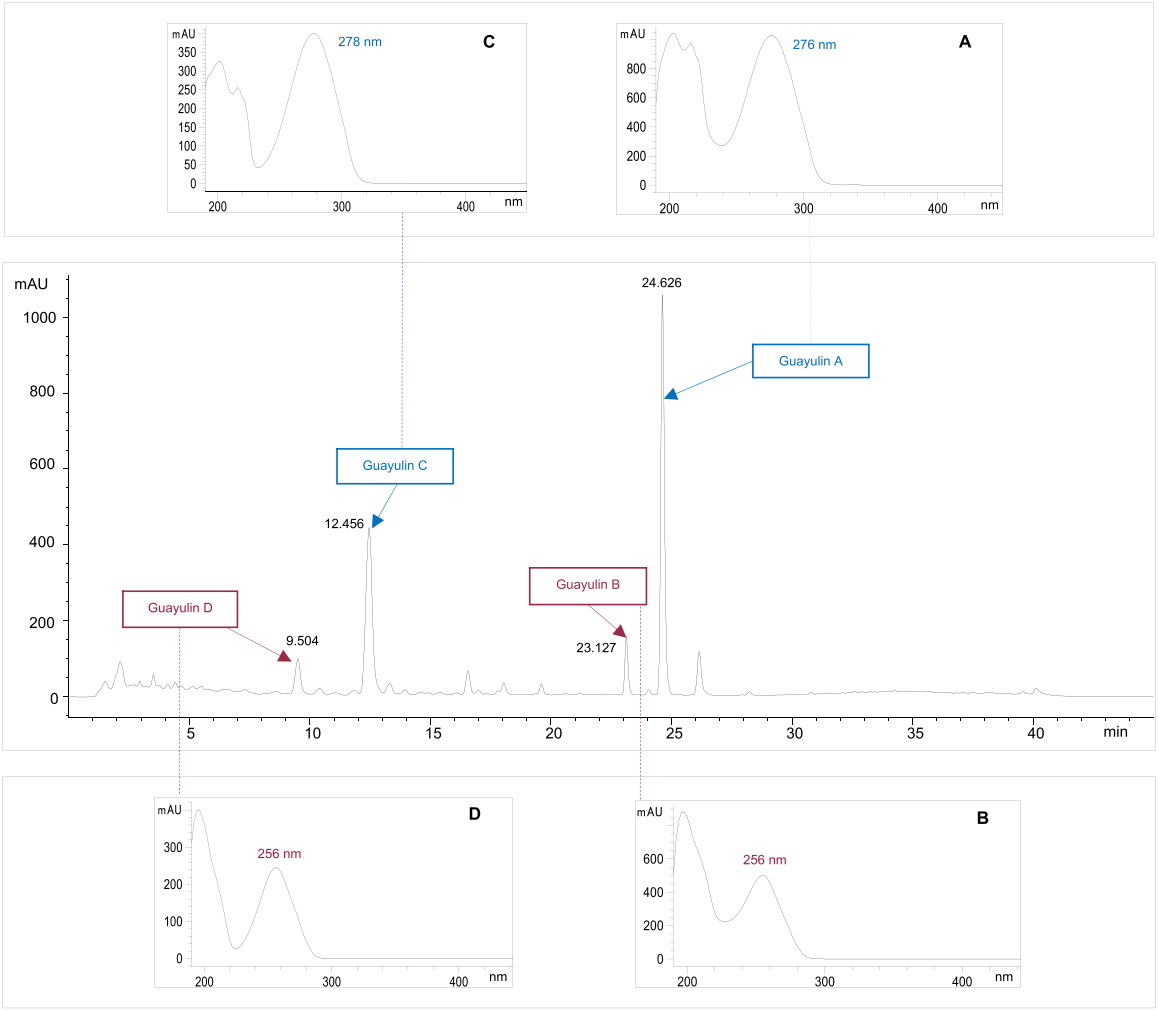

Fig. 2. Typical RP-HPLC-DAD chromatogram of resins from guayule (CAL-1 hybrid). Major guayulins identified with their corresponding UV spectra.

phenological phase, cultivar, age and shrub tissue (Sidhu et al., 1995; Teetor et al., 2009; Schloman et al., 1986). Of particular surprise is the seasonal difference in content reported by Scholman et al. (1986), specifically between sampling in January and July. The authors found that, although the resin content remained relatively constant per plant along the year (4.7–5.2 %), the variation in guayulin content was very large (27–3629 ppm for guayulin A and 5–526 ppm for guayulin B). The stem content decreased at the beginning of the year (January to February), and thereafter rapidly reached a maximum in March (3629 ppm for guayulin A). Our detailed analysis of guayulin content in two different accessions (CAL-1 and 11619) cultivated in Toledo, Spain, showed that guayulin content decreased significantly in the November sampling, which was not due to dilution or redistribution effects, as the plant did not generate more biomass during that stage (Fig. 3). Indeed, in November the plant is largely dormant, but still accumulates more resin. The increase in overall resin content, 80.5 % for CAL-1 and 39.2 % for 11619, does not, however, explain the sharp decline in the content of guayulins, which dropped below 40 % in both cases of the concentration in September. The decline in guayulin content does not reflect a dilution effect of the guayulins within the resin itself.

In addition of the decrease in the overall guayulin content, there was also a change in the relationship between the different guayulins. Both Teetor et al. (2009) and Sidhu et al. (1995) reported that the content of guayulin A is higher than that of guayulin B. Our results confirm this, but

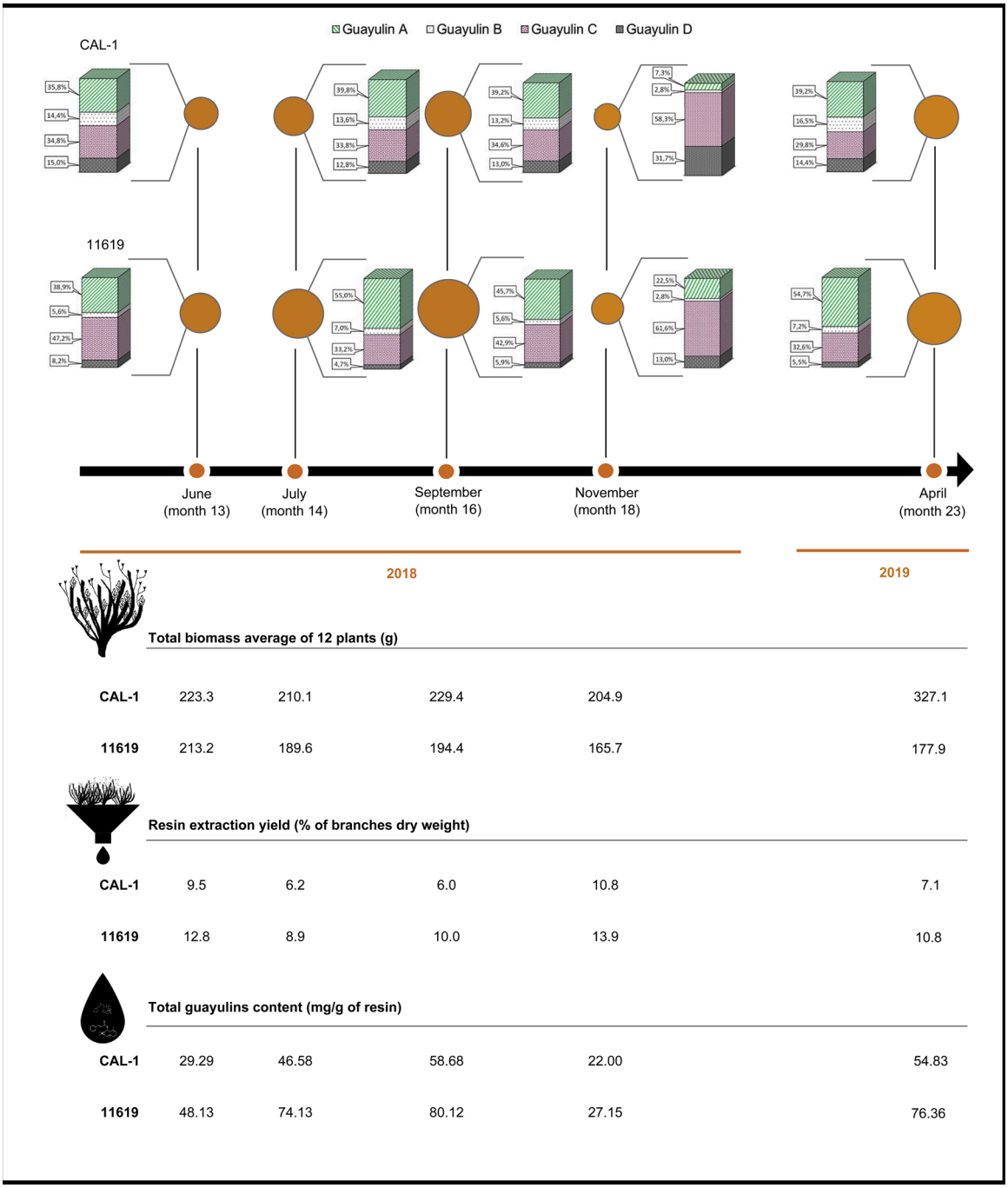

Fig. 3. Timeline evolution of total biomass, resin yield extraction and guayulin content in branches of CAL-1 and 11619 accessions from June 2018 to April 2019. NOTE: Orange circle represents proportionally the average amount of guayulins expressed in mg/g of resin at the bottom of the figure. Total biomass corresponds to the whole plant dried biomass expressed in grams.

we also found that the ratio between the two compounds differed depending on the genetic origin of the shrub: a lower ratio in the CAL-1 hybrid (between 2.4 and 3.0 for A over B) and a higher ratio in the much older 11619 accession (between 6.9 and 8.0) (Fig. 3). A similar but less pronounced pattern was found by Teetor et al. (2009). The ratio of guayulin A to B is much lower in the newly developed varieties AZ-1 and AZ-3 (between 3:1 and 5:1 depending on the thickness of the stem) than in the older variety 11,591 (20:1 to 40:1), which shares an origin with the accession 11619 used in our study (Ilut et al., 2017). Along this line, Teetor et al. (2009) hypothesized that the breeding regimen to endow plants with greater vegetative development has inadvertently caused substantial changes to the synthesis and accumulation of guayulins. These relationships can be used to guide breeding processes, as they are related to the genetic origin of the plant. The difference in the proportion of guayulins also depends on the plant tissue analysed. For example, Proksch et al. (1981) found that whereas guayulin A was 3–5 times higher than guayulin B in the stem, the ratio was essentially 1:1 in the leaves.

Guayulin A and B are thought to be cinnamate and *p*-anisate storage substances, with metabolic reversion when needed by the plant (Schloman et al., 1986). Cinnamic acid is involved in the biosynthesis of many important secondary metabolites in plants with roles as diverse as plant growth, reproduction or disease resistance. These secondary metabolites include phenyl-propanoids, coumarins, lignans, isoflavonoids, flavonoids, stilbenes, aurones, anthocyanins, spermidines, and tannins (Guzman, 2014).

Cinnamic-related molecules have attracted increasing attention because of their known biological activities, including anticancer, antituberculosis, antimalarial, antifungal, antimicrobial, antiatherogenic and antioxidant activities (Guzman, 2014). Some authors suggest that the defensive role of the sesquiterpene lactones, which are relatively abundant in some other plants of the genus *Parthenium* but are absent in guayule, is replaced by the guayulins in guayule, but for a slightly different purpose. While the sesquiterpene lactones are thought to defend plants from predators and pathogens, the guayulins, lacking oxygenated rings, would be directed to allow guayule to compete better with other plants (Mears and Larson, 1982). This is consistent with the allelopathic affects observed on eight different plant species caused by extracts from guayule residues containing cinnamic acid, related compounds, and compounds of the benzoic acid family (Schloman et al., 1991).

A comprehensive consideration of the whole family of guayulins, not only A and B, might shed more light on the synthesis, accumulation, and biological relevance of these compounds. As mentioned, the content of guayulins A and B seems to be related to the genetic origin and degree of hybridization. This notion led Sidhu et al. (1995) to propose that they be considered as unique biomarkers for breeding programs, as they are not present in any of the other species in the genus *Parthenium*. In first-generation hybrids obtained from guayule and other *Parthenium* species, the content of guayulins was between one-fifth and one-tenth that of the parental guayule (Proksch et al., 1981). This is not seen in well-established hybrids like CAL-1, which was analyzed in the present study (Fig. 3). We found that the content of CAL-1 guayulins at several sampling times (June, July, September) was lower than in the 11619 line, but not of the order of magnitude reported by other authors (Proksch et al., 1981).

It would seem reasonable to assume that there are more than four compounds belonging to the guayulin family. Teetor et al. (2009) reported that there may be other unique guayulins different from the major established compounds (A–D), and they reported a compound eluting immediately behind guayulin A from the AZ-1 and AZ-3 lines with a spectrum similar to that of the cinnamate chromophore in guayulin A. We also found this compound in the present study at 26.121 min (Figs. 2 and 4) together with other compounds that could be structurally related to guayulins by virtue of similar absorption spectrum characteristics. Interestingly, these compounds are found in greater quantity when guayulin A content decreased during the vegetative phase, as illustrated in the November sampling (month 18) in Fig. 4. Six potentially new compounds belonging to the guayulin family were found between 13 and 27 min, with absorption spectra similar to those of the known guayulins A, B and C (Fig. 4). Nevertheless, the unambiguous identification of these compounds will require considerable effort for their isolation and in-depth analysis, as they are found in small amounts. The process of identification of these potential new compounds could be similar to that for guayulins C and D, which were initially considered to be oxidation products of A and B, respectively, promoted by the increase in temperature (Schloman et al., 1983). It was later demonstrated that they were not extraction artefacts but were present naturally (Martínez et al., 1986).

Considering the analysis of guayulins C and D, which were not detected in the first characterization studies (Sidhu et al., 1995; Teetor et al., 2009; Schloman et al., 1986), their quantification in different varieties might reveal reasons for the seasonal variation in the A and B guayulins. Along this line, the first clue was offered by Spano et al. (2018), who found that guayulin C was in a higher proportion to guayulin B in leaves and, under some conditions, also in dried coarse stems, and had a content close to that of guayulin A in leaves. Depending on the solvent used for resin extraction – ethanol or acetone – the content of guayulin C reached between 65 and 81 % of the content of guayulin A, in leaves, which is a significant amount. The percentage of guayulin C was slightly lower than that of guayulin A in both accessions at the September stem sampling but changed dramatically at the next sampling (November) when the guayulin C content was much higher (Fig.3). As a result, we analysed the leaves of our plants in November and found that whereas guayulin A content dropped markedly in the stems, it was still present in a high proportion in the leaves (Fig. 5).

While the natural rubber content in the leaf is usually below 0.5 % (up to 2% according to Teetor et al., 2009), the resin content can vary between 8 and 12 % (Gilliland et al., 1984), suggesting that the leaves may be a viable source of concentrated guayulins. Their content can be in the order of 1700–1900 ppm (0.1–0.19 %), minor but of the same order of magnitude as their content in stems (Schloman et al., 1986). We found that the quantities of guayulin A and C depended on the overall guayulin quantity, as the striking 58.3 % guayulin C of total guayulins in November equated to a lower absolute amount since the total guayulin content decreased (Fig. 3), and the guayulin composition was very different in the leaves and stems (Fig. 5).

Spano et al. (2018) attributed the high presence of guayulin C and D in leaves to the exhaustive process of dehydration to which the leaves were subjected. In our case, the entire plant was dried at the same time, and the leaves were removed for analysis when the stems were completely dry (Fig. 5), so the high level of guayulins we describe is likely not an artefact of their extraction. By contrast, Spano et al. (2018) used a different approach: first separating the different fractions and freezing them, and then, just prior to analysis, drying the samples for different times until they reached a constant weight. It is also important to note that whereas the present study used cultivated accessions, Spano et al. (2018) studied wild guayule found in the Mapimi section of the Chihuahuan desert of Mexico.

In summary, sample processing likely does not account for the seasonal changes found by Schloman et al. (1986), the high content of guayulin C found by Spano et al. (2018), or the high guayulin C / A ratio described here. Overall, these results support the hypothesis that guayulins and natural rubber might share the same precursor (Arreguin et al., 1951; Gilliland et al., 1984). The biosynthesis of rubber in guayule is not fully understood, but it differs in some respects to other rubber-producing plants (Cornish et al., 2000; Cornish and Scott, 2005; Kajiura et al., 2018; Benedict et al., 2014). Several studies suggest that a precursor or promoter might be produced in the leaves (reviewed by Bhatia and Masohan, 1983), which then translocates to the stem and root parenchyma where the accumulation of natural rubber is high. Indeed, defoliation of plants before the cold season results in less rubber accumulation (Gilliland and van Staden, 1986). The reduction of stem guayulin A content in November, as rubber biosynthesis begins to

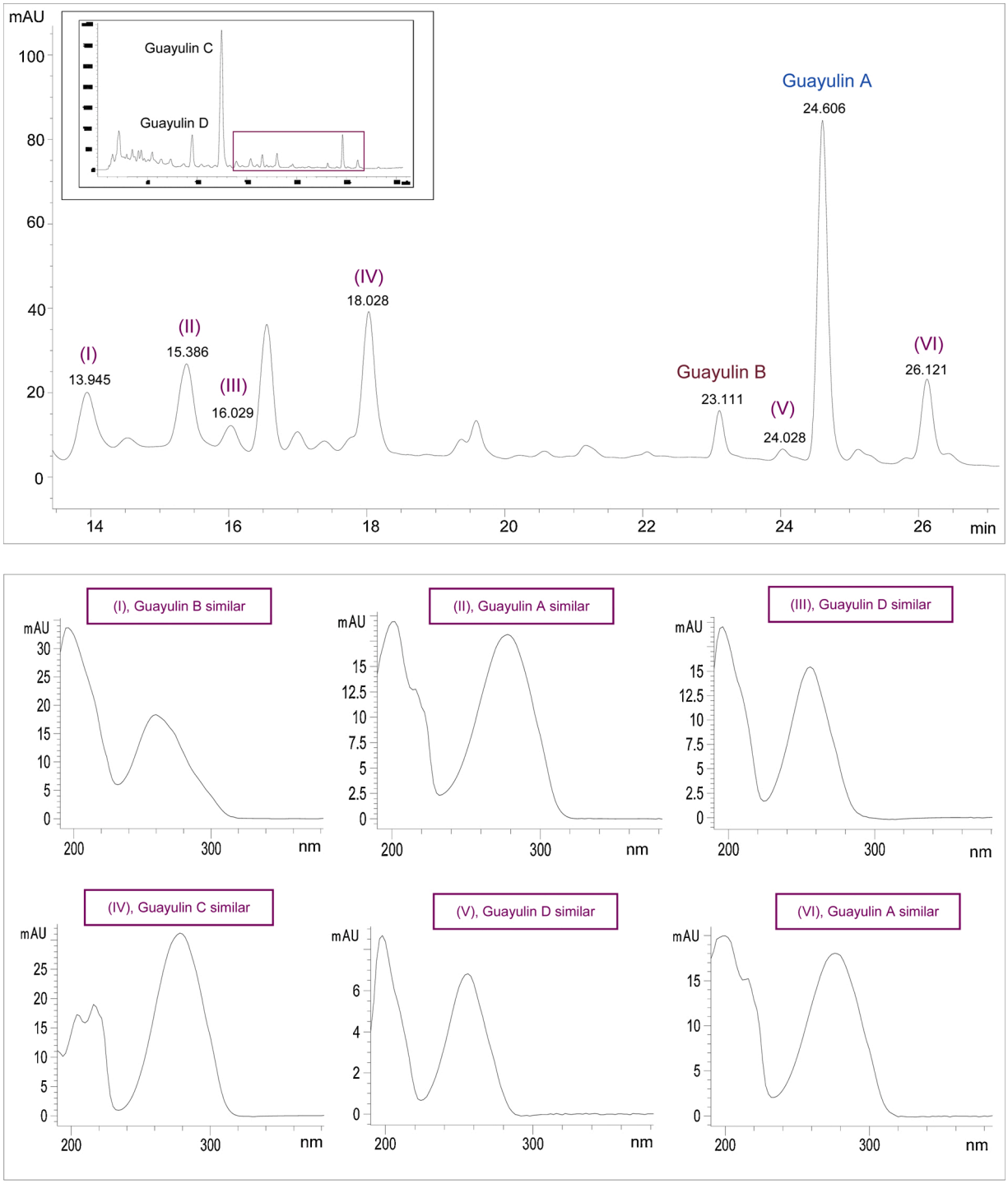

Fig. 4. Enlargement of the RP-HPLC-DAD chromatogram of the resin extracted from CAL-1 hybrid sampled in November. UV spectrum of the minority peaks.

increase, might suggest that it is involved in the biosynthesis of natural rubber. This hypothesis would fit well with the recent demonstration that rubber particles are generated in the epithelial cells surrounding the resin channels of the stem and roots as well as in the bark parenchyma. These cells are bifunctional in nature, and remodel by organelle decomposition to accumulate rubber particles (Kajiura et al., 2018).

Teetor et al. (2009) performed a detailed analysis of the content of guayulin A and B in eight different parts of the plant from three varieties of guayule (11,591, AZ-1 and AZ-3), and found that the proportion of guayulin A was greatest (30.9–38.4 %) in the stems of larger diameter (>1 cm), reaching 14.3 % of the dry weight of these stems – which are also the part of the plant that accumulates most rubber. Their findings for the months of October and April are in accord with our findings of a high content of guayulin A in September and April (Fig. 3). These data are in good agreement with the seasonal variations in rubber production: high production in autumn, when night temperatures are around 7 °C (Ji et al., 1993), which is sufficiently cold to stimulate the accumulation of natural rubber; and low production in spring, when the plant has already started vegetative growth and is accumulating guayulins. In both cases, the content of guayulin A in the stems is high. Guayulin A

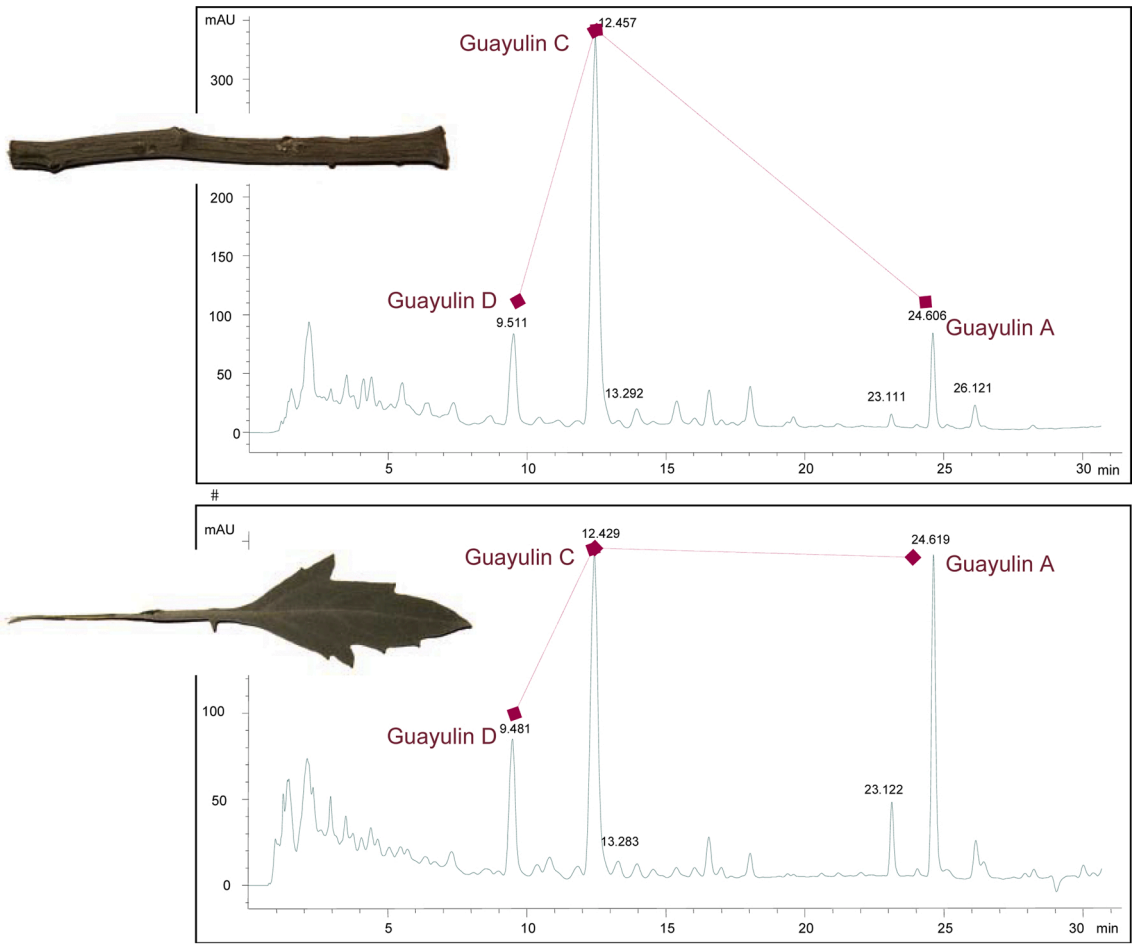

Resin extraction yield (%) Expressed as percentage of the dried biomass	Guayulin content expressed as mg of guayulin / g of resin			
	Guayulin D	Guayulin C	Guayulin B	Guayulin A
10.8	7.02	13.09	0.43	1.46
7.8	6.86	6.91	2.43	3.61

Fig. 5. Comparison of guayulins content in the same CAL-1 cultivar in the stems and leaves after 18 months growing (November).

declines a little later (November) when the biosynthesis and accumulation of natural rubber is activated. This occurs in the stems, but the concentration is higher in the leaves (Fig. 5).

Comparing the agronomic behavior of guayule and the accumulation of secondary products in different environments is challenging, especially as guayule lines are not genetically homogenous. At the very least, the same lines should be tested together in different soils and climatic conditions. Comparisons between sampling dates must be performed carefully and with a broad time window. When this is done in relation to guayulins, specific seasonal changes can be found consistently across different research groups (Schloman et al., 1986; Teetor et al., 2009; Coffelt et al. 2009). Also, when the content of guayulins A and B was analyzed in lines AZ-2 and 11,591 over 1.5 years, including two consecutive November months, the evolution over time was very similar (Coffelt et al. (2009), Table 2). This occurred even though: 1) the amount of guayulin A (in grams) that accumulates in the accession 11, 591 is much higher than that in AZ-2; 2) the opposite occurs for guayulin B in these lines (Table 2).

As reported by Coffelt et al. (2009), although the plants were already 20 months old, the initial content of guayulins in November 2002 was very low, but increased considerably through March 2003 and continued to increase until July 2003. By November 2003, the content was essentially stable, increasing only slightly with respect to the previous July. Some parallels can be drawn between the results of Coffelt et al. (2009) and our findings (Fig. 3). We continued sampling until September to assess whether the content of guayulins, in general, and guayulin A and B, in particular, continued to increase. Although detailed inter-study comparisons are not possible because of site differences, the levels of guayulin A and B consistently dropped during the winter season (Coffelt et al. 2009 and Fig. 3) as rubber content increased.

Table 2
Content of guayulin A and B in two guayule accessions between November 2002 and July 2004. Elaborated from Coffelt et al. (2009).

		Content *versus* previous sampling					Initial content (g per g of resin)	Final content (g per g of resin)
		March 2003 *vs* Nov. 2002	July 2003 *vs* March 2003	Nov. 2003 *vs* July 2003	March 2004 *vs* Nov. 2003	July 2004 *vs* March 2004	Nov. 2002	July 2004
Guayulin A								
	11,591	475 % [a]	283 %	102 %	86 %	164 %	0.60	11.54
	AZ-2	428 %	209 %	110 %	88 %	252 %	0.18	3.91
Guayulin B								
	11,591	500 %	264 %	107 %	81 %	160 %	0.02	0.40
	AZ-2	413 %	216 %	117 %	90 %	216 %	0.05	0.93

[a] The percentage represents the content at this harvesting time compared with the preceding sampling (formula = current content/previous content *100). A percentage greater than 100 % indicates that the guayulin content increased in the last period of, whereas a percentage less than 100 % indicates a decrease in content. To the right of the table are the values between the first and last sampling points to provide the scale for each of the guayulins and accessions.

Additional studies are needed to prove or disprove a direct relationship between guayulins and rubber biosynthesis. It might that rubber biosynthesis *per se* starves the more downstream guayulin pathway of precursors by its consumption of isopentenyl pyrophosphate. Alternatively, it may involve identifying an "unknown precursor", to establish the full pathway and to characterize the enzymes involved, which is not an easy task (Benedict et al., 2014). An indirect way would be to analyze, in-depth, the profile of this family of compounds in many varieties and throughout the whole growth cycle, and to corroborate that there is a similar, opposing pattern of accumulation for guayulins and rubber. Several authors have attempted to relate the rubber content to either the resin content or the guayulin content, with contradictory results (Thompson et al., 1988; Luo and Abdel-Haleem, 2019). This might be because their relationship changes with season and development stage. Guayulins accumulate throughout most of the year while rubber production is enhanced at cold/cool temperatures (Ji et al., 1993).

Nevertheless, performing these determinations would be useful to establish if, as suggested, they can be used as biomarkers in the breeding process (Sidhu et al., 1995) and also to clarify the function of guayulins in the plant, and their possible participation – directly or indirectly – in the biosynthesis of natural rubber.

3.2. Technical improvements in characterization and isolation of guayulins

The results and correlations discussed in the previous section were obtained by using HPLC and UV detection. In this section, we critically evaluate alternative methods for guayulin and resin analysis, identification and quantification.

3.2.1. Liquid chromatography–mass spectrometry

LC–MS can resolve all four guayulins (Fig. 6) in less than 10 min. with complete precision, partly because perfect chromatographic separation is not required when mass detectors are used. The increase in chromatographic efficiency is achieved by the use of smaller columns and smaller particle sizes than used for HPLC-UV and allows a reduction in analysis time and solvent consumption. While LC–MS equipment may not be affordable to all researchers due to its capital cost, the small volume of solvents required can mitigate the initial expense and lead to considerable savings in solvents over time; in this case by two and a half times (15 mL *versus* the 37.5 mL mobile phase used by Spano et al., 2018).

The characteristic of *m/z* peaks at 105.1 and 147.1 corresponding to C_8H_9 and $C_{11}H_{15}$, respectively, (Fig. 7) are present in the spectra of all four guayulins (Fig. 6), allowing them to be accurately quantified even when they partially overlap with other compounds. In addition, their spectra show signals from the ester groups (red colour, Fig. 6) and from the central nucleus of the molecules (blue colour, Fig. 6). Cinnamic and *p*-anisic acid moieties can be easily differentiated by the signals they provide when the ester bond is broken, losing the hydroxyl group, which remains attached to the isoprene structure. The *m/z* value 131.0 corresponds to $[trans\text{-cinnamic acid } -OH]^+$ while the *m/z* value 135.0 corresponds to $[p\text{-anisic acid } -OH]^+$ (Fig. 7). After fragmentation, the bicyclogermacrene structure (guayulin A and B) shows characteristics *m/z* signals of 149.1, 161.1 and 203.2, corresponding to $C_{11}H_{17}$, $C_{12}H_{17}$ and $C_{15}H_{23}$, respectively. In contrast, the aromadendrene structure (guayulin C and D) breaks into fragments with two less hydrogen atoms: *m/z* values of 147.1, 159.1 and 201.2 (Fig. 7). Guayulins C and D have an additional spectral line of *m/z* value 219.2 corresponding to $C_{15}H_{22}O$ (Martínez et al., 1986), as the isoprenoid ring has one more hydroxyl group in position C4 when separated from the *trans*-cinnamic acid or *p*-anisic acid substitute (Fig. 7).

Tracking the full scan mass spectrum for the exact mass 351.2319, in search of the possible compound mentioned by Teetor et al. (2009) with a UV absorption pattern similar to guayulin A, we found a peak (retention time 6.62, Fig. 8) that, depending on the variety and time of harvest, could be even higher than that for guayulin A (retention time 7.83, Fig. 8).

This new peak had the same mass and molecular formula as guayulin A, but presented a cleaner fragmentation, with a smaller number of scan lines that were also more similar to those for guayulins C and D (147.1, 159.1 and 201.2) than to those for guayulin A itself (Fig. 8). We speculate that this is actually maali-3-en-8α-ol-cinnamic ester, because the extra bond in the center of the isoprenoid nucleus would make it more resistant to fragmentation. This compound would be formed from maali-3-en-8α-ol, identified for the first time by Maatooq (2002) while studying the microbial transformations of partheniol by *Mucor circinelloides*, and by *trans*-cinnamic acid, the typical precursor of guayulin A. Maali-3-en-8α-ol is generated spontaneously in acid medium by transannular cyclization between the C-10 and C-5 of partheniol without the need for enzymatic catalysis (Asakawa and Noma, 2010). More detailed studies will be necessary to confirm this speculative identification and also to determine the structure of the other minor guayulins evident in guayule resin.

3.2.2. Matrix-assisted laser desorption ionization–time-of-flight mass spectrometry

There are even faster methods than LC–MS that could be applied for the detection of guayulins, which do not even require the chromatographic separation phase. Time-of-flight mass detectors introduce the sample either by means of a matrix that helps in the ionization carried out by a laser (MALDI) or by means of electrospray (ESI) of a solution containing the compounds to be studied. MALDI-TOF mass spectrometry is now a routine analytical tool for the identification of microbial species by their characteristic protein profiles (Hou et al., 2019) and for the structural analysis of polymers (Wu et al., 2017). It requires very simple sample preparation once the working conditions are established (Payne and Grayson, 2018), and takes just a few minutes to generate results.

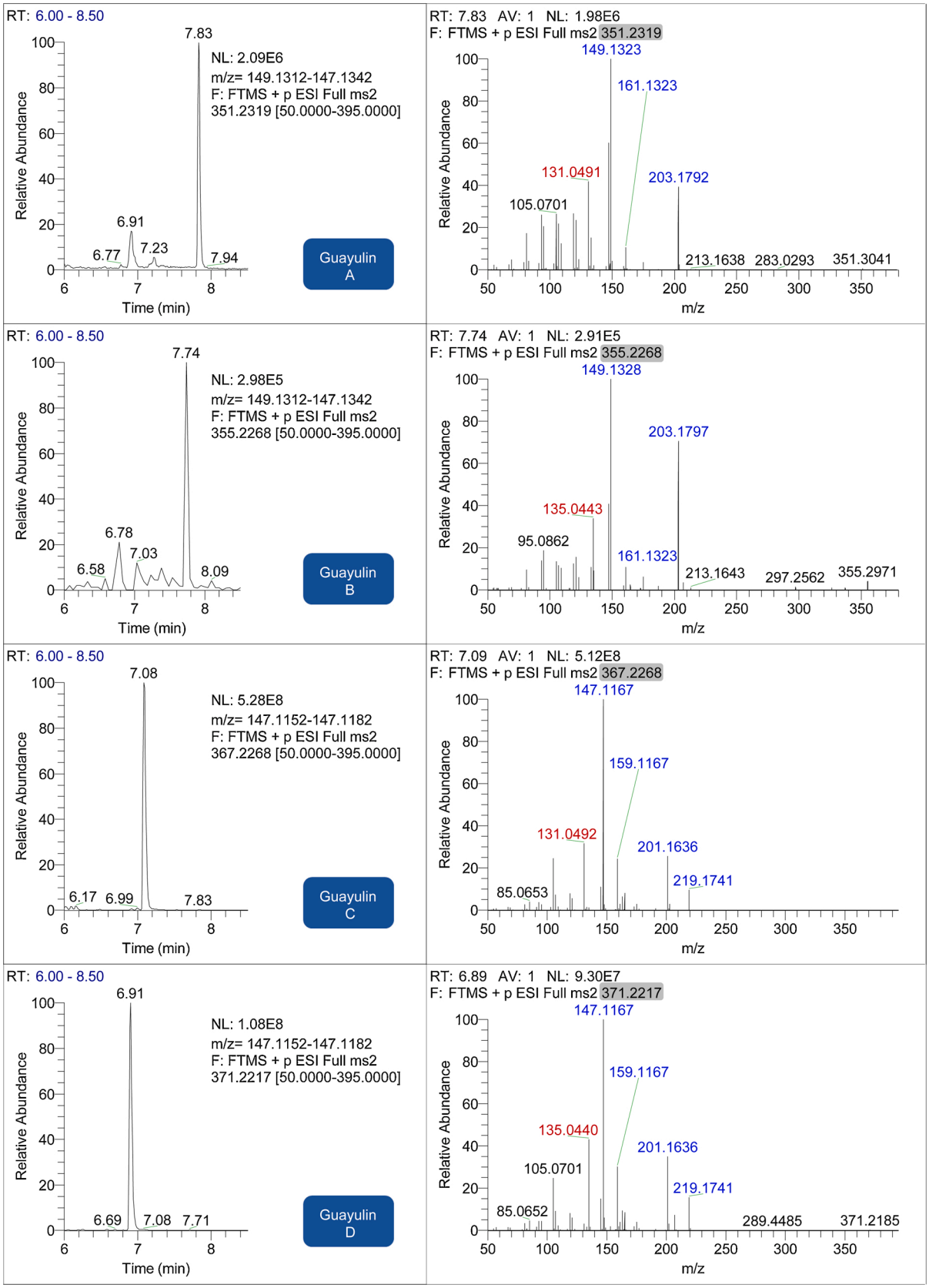

Fig. 6. LC–MS/MS analysis of the following four *m/z* values: 351.2 and 355.2, 367.2 and 371.2, corresponding to $M+H^+$ of : (a) guayulin A, (b) guayulin B, (c) guayulin C and (d) guayulin D, respectively.

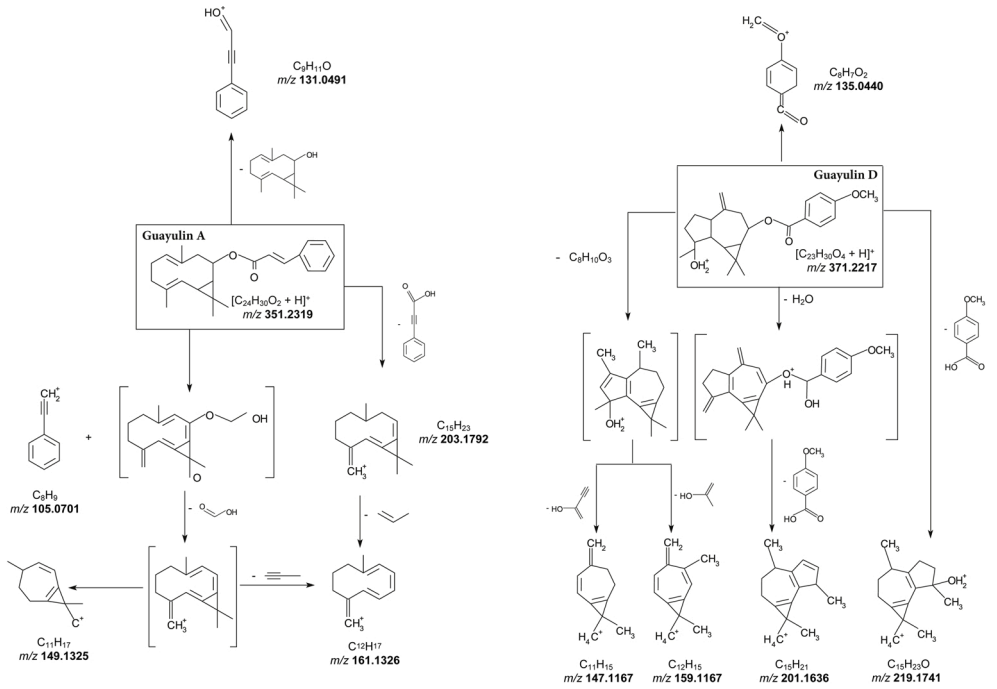

m/z	105.0701	131.0491	135.0440	147.1167	149.1325	159.1167	161.1326	201.1636	203.1792	219.1741
fragment	C_8H_9	C_9H_7O	$C_8H_7O_2$	$C_{11}H_{15}$		$C_{12}H_{15}$	$C_{12}H_{17}$	$C_{15}H_{21}$	$C_{15}H_{23}$	$C_{15}H_{23}O$
δ (ppm)	2.62	0.64	-0.59	-0.66		-1.09	-0.80	0.93		1.58
Guayulin A	X	X		x	X		X		X	
Guayulin B	X		X	x	X		X		X	
Guayulin C	X	X		X		X		X		X
Guayulin D	X		X	X		X		X		X

Fig. 7. Detailed explanation of guayulin fragmentation.

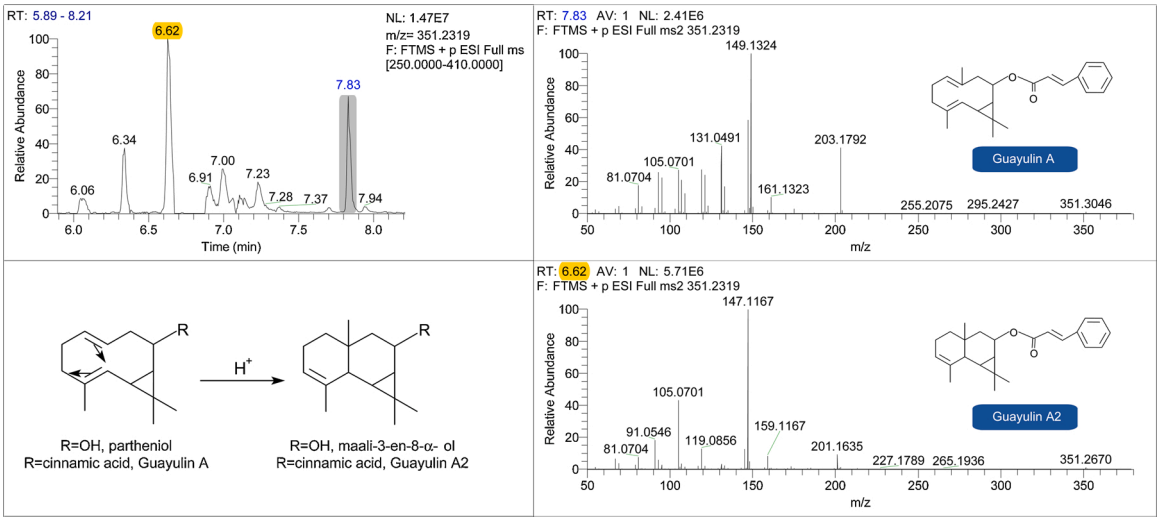

Fig. 8. Suggested structure for guayulin A_2.

A limitation of MALDI-TOF for guayulin analysis is its ability to detect small compounds in the molecular weight range 300–400 Da. The ionization of the matrix produces noise in this range and reduces detection sensitivity. Nevertheless, MALDI-TOF has been used to characterize low molecular weight guayule rubber (LMWGR) from guayule (Chiang et al., 2014), which are often ignored when rubber is analyzed for industrial interest (industry is interested in the largest polymers). The authors found that 54 % of the rubber is low molecular-weight rubber, although this level decreases to 27–31 % in purified rubber particles. According to Zoeller et al. (1994), LMWGR is also co-extracted during the acetone extraction of guayule to obtain resins or isolated guayulins. Fig. 9 illustrates the MALDI-TOF results when analyzing the guayule resin after extraction with acetone, according to section 2.2.

A polymeric structure is observed with a repeated pattern that decays exponentially towards 4000 Da (Fig. 9a), when the acetone extraction is performed by ASE at 40 °C, as described (Suchat et al., 2013), consistent with multimers of the isoprene unit (68 Da). The content of LMWNR in the resins can be high, around 15 % of the resins (Cheng et al., 2020) and

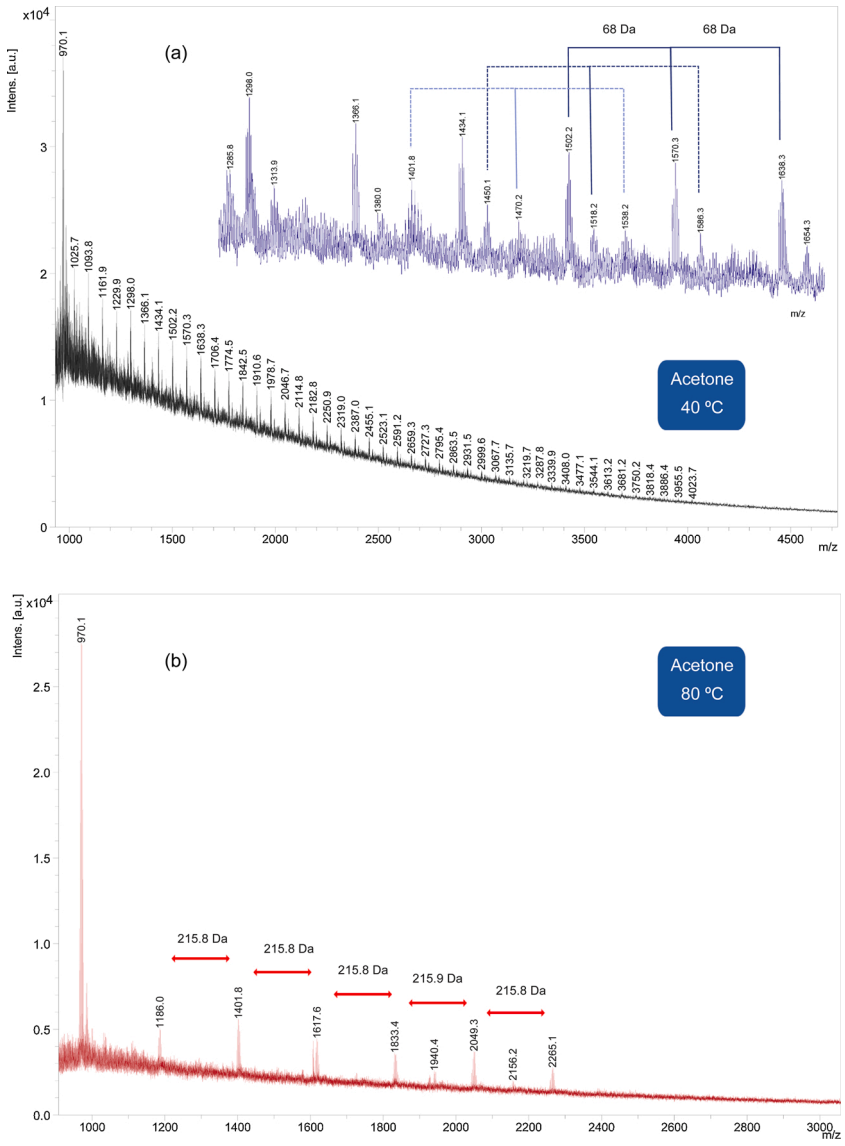

Fig. 9. MALDI-TOF analysis of guayule resins extracted with acetone at 40 °C and 80 °C from 900 to 5000 Da.

between 1–2 % of the dry weight of the plant (Meeks et al., 1950), a concentration that can vary considerably depending on the method of extraction. The low yield of high molecular weight natural rubber in exhaustive extractions of plants with high resin content is attributed to the degradation of rubber under these conditions (Salvucci et al., 2009), resulting in smaller molecules. The same is observed when acetone is used at a higher temperature (80 °C) in ASE extraction of resins (Fig. 9b). The constant pattern of 68 Da (the size of the isopentenyl rubber monomer) is lost and becomes about 216 Da, the size of the polymers doesn't match with the extracted at 40 °C (Fig. 9a) and many molecules sizes are no longer present within the new range (Fig. 9b).

According to Zoeller et al. (1994), the presence of LMWGR makes it difficult to isolate the most non-polar compounds, guayulins A and B, by chromatography. During their extraction with acetone, not only was LMWGR co-extracted, but also a significant amount of water (20 %), which may contain polar compounds that absorb in the UV spectrum and make guayulin determination challenging (Zoeller et al., 1994). To remove both LMWGR and water, the authors proposed dissolving the resins in ethyl acetate, washing with a brine solution, then separating the organic phase from the water and the semi-solid precipitated LMWGR. To ensure that this cleaning process functions as intended, it would be useful to employ reverse-phase HPLC-UV to confirm that the best conditions for extracting guayulins are chosen and, in parallel, to use MALDI-TOF to minimize interference by any remaining LMWGR.

3.2.3. *Electrospray ionization–time-of-flight mass spectrometry*

The simple and fast data acquisition by time-of-flight spectrometers can be exploited to determine small, relatively polar molecules like guayulins using direct probe ESI, as long as the mixture is not excessively complex (Figs. 10 and 11).

The differences in the mass fragmentation patterns for guayulins in LC–MS (Fig. 6) and ESI-TOF (Fig. 10) are not due to the ionization form, as both instruments use ESI to introduce the solubilized sample into the mass spectrometer, and both include formic acid to favor the appearance of the $M+H^+$ adduct. Rather, the differences reflect the presence and absence of chromatography, respectively. Chromatography, a purification technique in itself, allows the elimination of free Na^+ by the use of RF-C_{18} columns at the moment the drop is formed just before ionization. Together with the presence of formic acid in the mobile phase, this ensures that the $M+H^+$ adduct is greatly favored. This is not the case when using ESI-TOF because no previous separation is performed and everything in the sample is analyzed together. The content of Na^+ ions in guayule latex is surprisingly high when compared with the content in *H. brasiliensis* latex (Cornish et al., 2012). Accordingly, during the

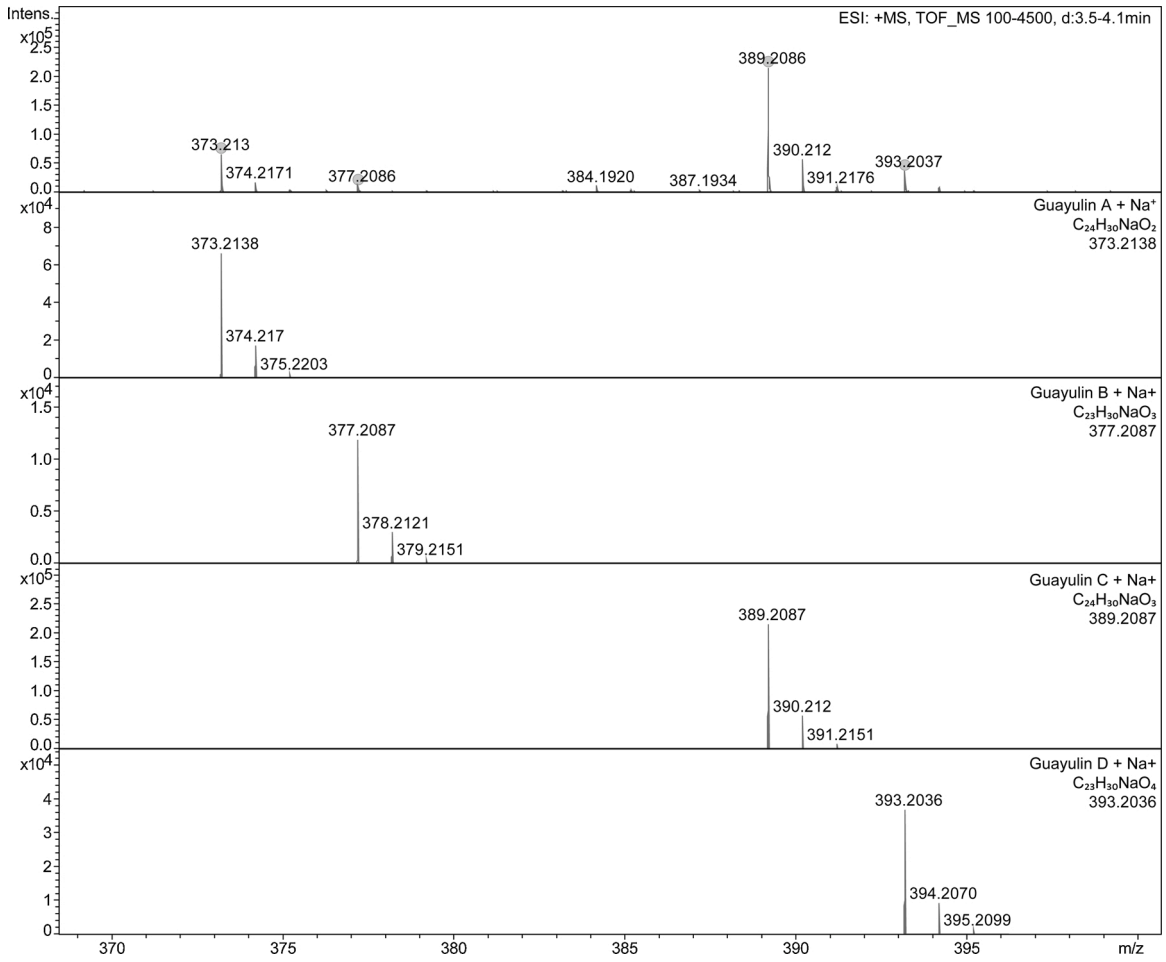

Fig. 10. ESI-TOF analysis of guayule resin.

acetone extraction process step a large quantity of Na^+ salts, presumably organic forms, are obtained. These ions will later form adducts with Na + in the mass spectra of the guayulins with *m/z* values of 373.2, 377.2, 389.2 and 393.2 (Fig. 10).

For the same reason, in the MS/MS assays (Fig. 11) high intensity spectral lines appear in the fragmentation of the main ions. For example, the *m/z* value of 241.2 ($C_{15}H_{22}NaO$), which is predominant in the mass spectra of guayulins C and D, correspond to Na^+ adducts of spectral lines appearing in LC–MS with *m/z* values of 219.2 (Fig. 8). As expected, these additional spectral lines of Na^+ adducts are more evident in the more polar compounds, guayulins C and D. However, the presence of the Na^+ ion also promotes a different fragmentation in which extra signals appear at *m/z* 139.1, 171.0, 175.0, 261.2 or 277.2, which would correspond to molecular formulas of $C_6H_{12}NaO_2$, $C_9H_8NaO_2$, $C_8H_8NaO_3$, $C_{15}H_{26}NaO_2$ and $C_{15}H_{26}NaO_3$, respectively.

In summary, the ESI-TOF technique has proven to be very amenable for analyzing guayulins directly in the resin without any isolation or purification process. It remains to be seen, however, whether the technique can be used directly for the quantification of guayulins, which would require cross validation with the LC–MS determination.

This same idea, specifically, a raw analysis of the compounds in the resin avoiding the potential degradation of compounds present during fractionation, has been very recently performed by Cheng et al. (2020) using high-resolution Fourier transform ion cyclotron resonance mass spectrometry (FT-ICR MS). The results illustrated the great diversity of compounds present in the resin than previously seen. Indeed, they found that up to 7200 compounds might be present when the spectrometer is used in negative-ion mode, and 3500 in positive-ion mode. In relation to guayulins, the following conclusions can be drawn from the results presented in negative-ion mode: 1) they present an unusual pattern, as there is no large difference in the intensity of the *m/z* lines; 2) the intensities of the scan lines corresponding to guayulin A and C, and those of B and D are very similar; 3) the relative intensity of their *m/z* lines is much lower than those corresponding to the other relevant family of terpenes, the argentatins.

There are at least two possible explanantions for the unusual profile observed by Cheng et al. (2020), where the intensity for guayulin A (the majority) is similar to that for guayulin C and about double that for guayulin B and D. As the authors caution, the resin was not extracted from a single variety, but from a mixture of varieties; thus, the pattern might be due to the heterogeneity of the varieties. The second explanation is that the treatment of the resin in the pilot plant was so exhaustive that it caused the oxidation of A to C and of B to D, giving rise to the similar quantities. The difference between guayulins and argentatins is more difficult to explain. Although some authors have reported higher concentrations of argentatins (27 %) than guayulins (10–15 %) (Schloman et al., 1983), the proportion is unlikely to be as exaggerated as that reported by Cheng et al. (2020). One hypothesis is that the negative-ion mode promotes the preferential ionization of argentatins over guayulins. This preferential ionization of the positive-ion mode was seen (Cheng et al., 2020) for C_{12-15} hydrocarbon compounds and for compounds with two oxygen atoms (*e.g.*, guayulin A). We employed ionization in positive-ion mode when we utilized mass spectrometry for the determination of guayulins since it was the mode used by other researchers (Martinez et a., 1986), and also for argentatins (Maatooq, 2003). We compared the same sample in both modes, positive and negative, and confirmed that this was possibly one of the reasons for the difference in intensity between the scan lines of both families of terpenes

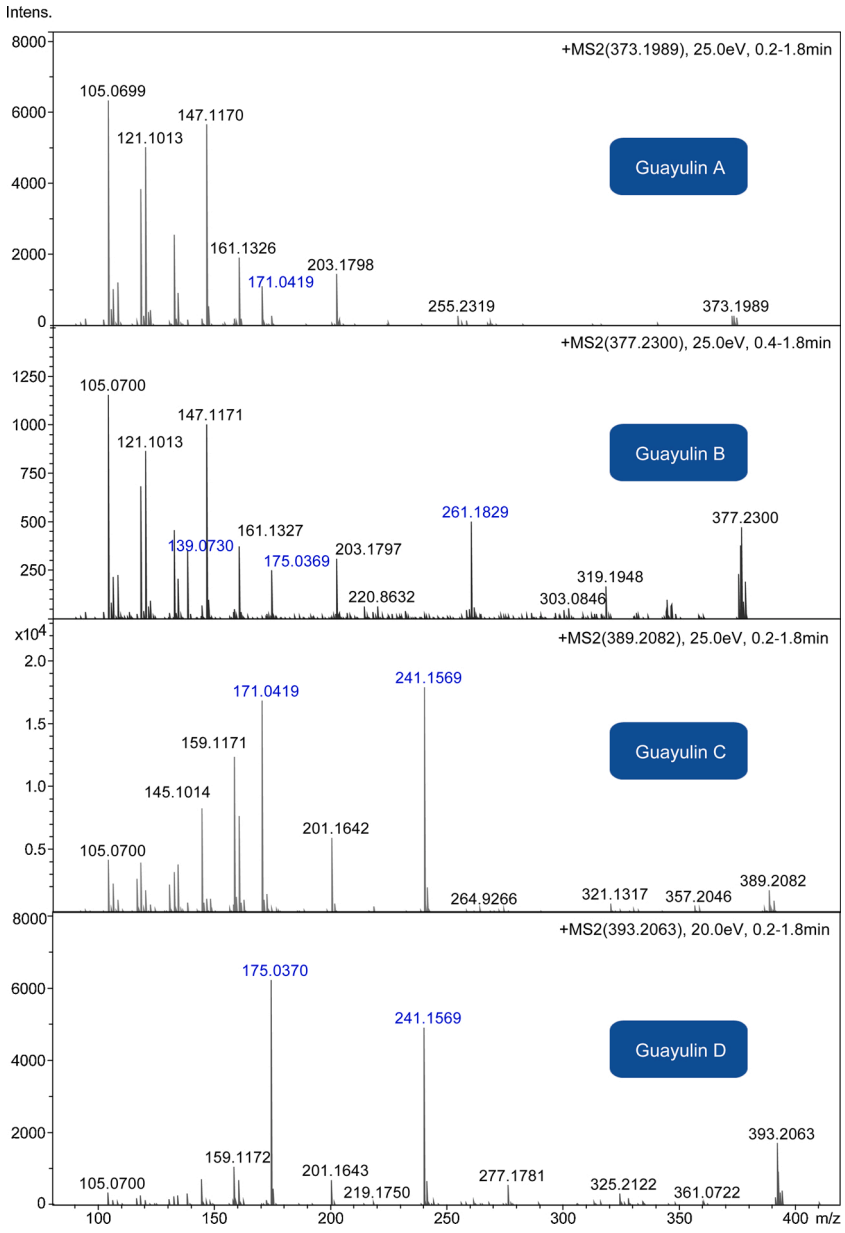

Fig. 11. ESI-TOF exact mass fragmentation experiment (MS/MS) of the following four *m/z* values: 373.2 and 377.2, 389.2 and 393.2 corresponding to: (a) guayulin A, (b) guayulin B, (c) guayulin C and (d) guayulin D plus Na^+ respectively.
NOTE: The adducts formed with Na^+ ion are highlighted in blue.

(Fig. 12). Indeed, Fig. 12 shows examples for the 3 guayulins and the 3 argentatins with the highest representation also using ICR-MS technology (Orbitrap®) after chromatographic separation. When comparing the intensity levels for the guayulins in positive-ion mode (numbers highlighted in gray, Fig. 12) with those in negative-ion mode (numbers highlighted in violet, Fig. 12) there are differences of about 3 orders of magnitude for the signals corresponding to the structure of guayulin A ($C_{24}H_{30}O_2$), that is, the compounds ionize 1000× better in the positive-ion mode than in the negative-ion mode. This was somewhat less for guayulin C and even more so for guayulin D. The signals obtained for guayulin A and guayulin D in negative-ion mode can be considered noise because of their insignificant intensity (10^4). The analysis of guayulin C in positive-ion mode allows the identification of a greater number of peaks (retention time 5.62, 6.17, 6.84) in addition to the majority (retention time 7.12), which could correspond to different isomers. In contrast, the negative-ion mode reveals two peaks that do not appear in the positive ionization (retention time 7.17 and 7.24), although this should be interpreted with caution as both of these peaks are much smaller than any of those appearing in the positive mode.

When we made the same comparison of argentatins, we observed that: 1) better ionizations were still obtained for compounds in positive-ion mode; 2) but the differences were not so great, with intensities 100× times higher in the major case (argentatin B); 3) some compounds ionized equally well in both modes (*e.g.*, peak retention time 6.88 in argentatin A) while others only appeared in one of the two modes (retention time 7.54 in negative-ion mode in argentatin A or the compounds of retention time 6.39, 6.51, 6.62, 6.70 in the search for *m/z* signals corresponding to the structure $C_{30}H_{38}O_3$ of argentatin B in positive-ion mode). Two compounds were identified for this structure: argentatin B and isoargentatin B (Romo de Vivar et al., 1990). As suggested by Cheng et al. (2020), ICR-MS technology can be an excellent tool to search for new compounds. This can be observed in the chromatogram in Fig. 12 for argentatin B in positive-ion mode, and there could be many more isomers than those known thus far.

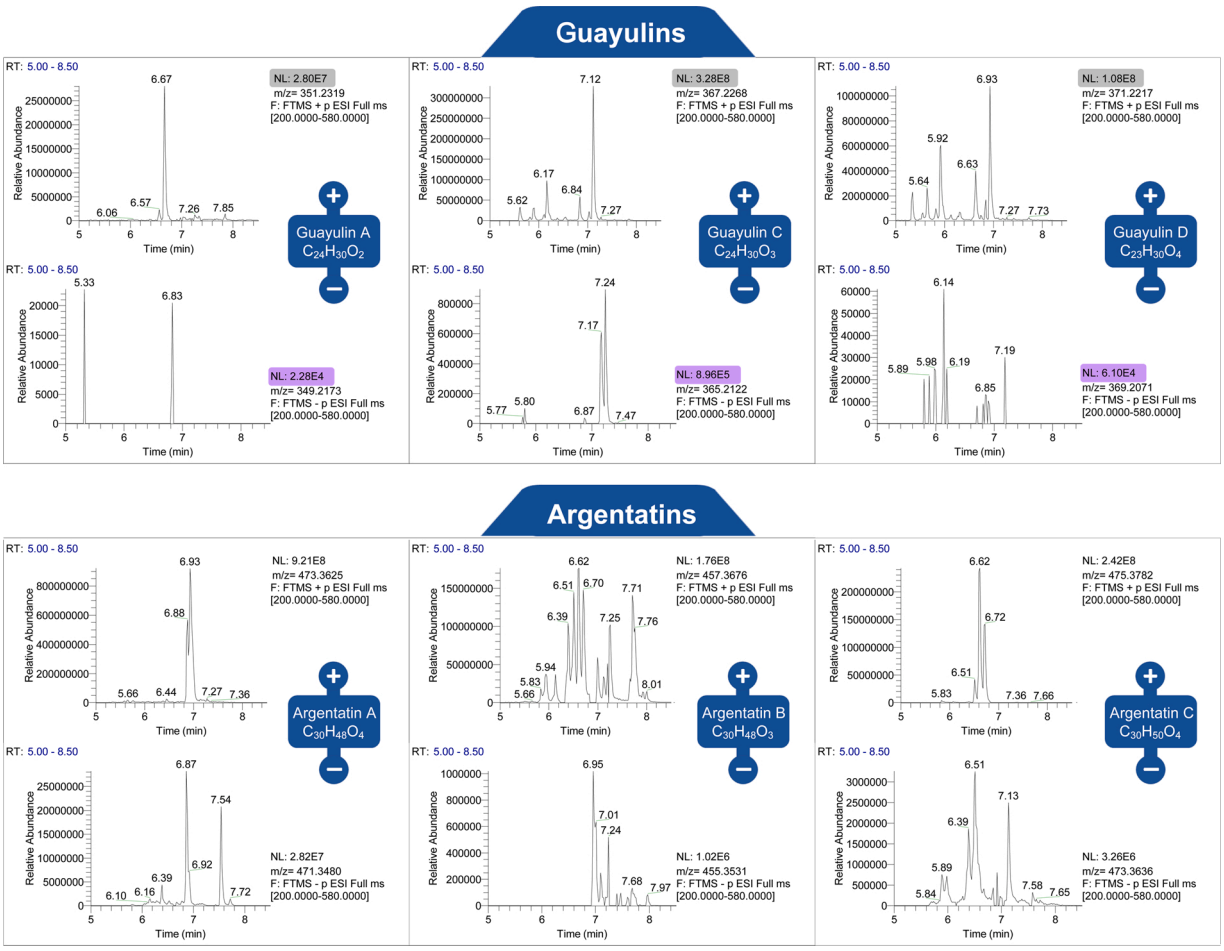

Fig. 12. Comparison of the ionization of the three main guayulins and argentatins in the same CAL-1 resin sample by positive-ion and negative-ion mode operation using an Orbitrap® mass spectrometer (FT-ICR-MS) after chromatographic separation.

For the above reasons, we suggest that the positive-ion mode be used in mass spectrometers for the determination of guayulins separately or in conjunction with argentatins. The guayulins have proven to be easily ionized in positive-ion mode. In fact, high energies are not required to achieve good fragmentation during MS/MS analysis (Fig. 13) and 10 or 20 V are sufficient to obtain abundant fragmentation that allows the compounds to be readily identified. Higher energies (30–70 V) cause excessive fragmentation with the consequent generation of very small *m/z* signals (105.0701, 119.0856, 91.0547) that mask the characteristic signals of the central nucleus; signals such as the 219.1740 typical of guayulin C and D, or others that characterize the family, such as 147.1167 or 201.1635 (Fig. 13 and Fig. 7).

In summary, using either of these spectrometry-based methodologies (ESI-MS, FT-ICR-MS) allows the simultaneous quantification of compounds of both families, guayulins and argentatins. In the best-case scenario, studies have presented two members of each family for a few varieties or conditions, while using two different methods of analysis (Schloman et al., 1986). By using the positive-ion mode, a smaller number of compounds can be identified, as suggested by Cheng et al. (2020) and verified in the present study where fewer *m/z* signals appeared (Fig. 14). If the aim is to analyze both families of compounds simultaneously, this option should be chosen, since the relationship between the intensities of the scan lines belonging to both families is much more balanced. For example, the intensity of the *m/z* line for the major argentatin (argentatin A, Fig. 14b) is about four times higher than that for the guayulin with the highest concentration (guayulin C, Fig. 14a), with values much closer than those obtained with the negative-ion mode (Cheng et al., 2020).

4. Conclusion

New analytical techniques that have not yet been extensively applied to the determination or characterization of guayulins can be very useful and can identify new members belonging to this family. Indeed, a new compound belonging to this family, maali-3-en-8α-ol- cinnamic ester, has been tentatively identified and there are clear indications that several more may exist. Further study of potential candidates will be needed to confirm this.

These techniques will be useful to simultaneously analyze the two largest families of terpenes (argentatins and guayulins) in guayule resins. To the best of our knowledge, there are no reports in the literature on the quantification of both families at the same time, nor variation caused by genotype or agricultural management.

More should be done to improve our knowledge of the secondary metabolism in guayule. The three advantages of speed, lower solvent consumption and unequivocal identification should encourage researchers to implement LC–MS analysis for routine analysis of guayulins. If this is not possible, and simpler UV detectors are still utilized, shorter columns with smaller particle size and higher pressures should be used for UHPLC, which is currently not much more expensive than conventional HPLC.

The present study together with the recent work of Cheng et al. (2020) should extend mass spectrometry analysis to raw samples without a prior separation process, useful in the direct analysis of both families, and would save time and money. We suggest that mass spectrometers be used in the positive-ion mode with low voltages for this purpose. Comparative tests made with multiple techniques (ESI-MS,

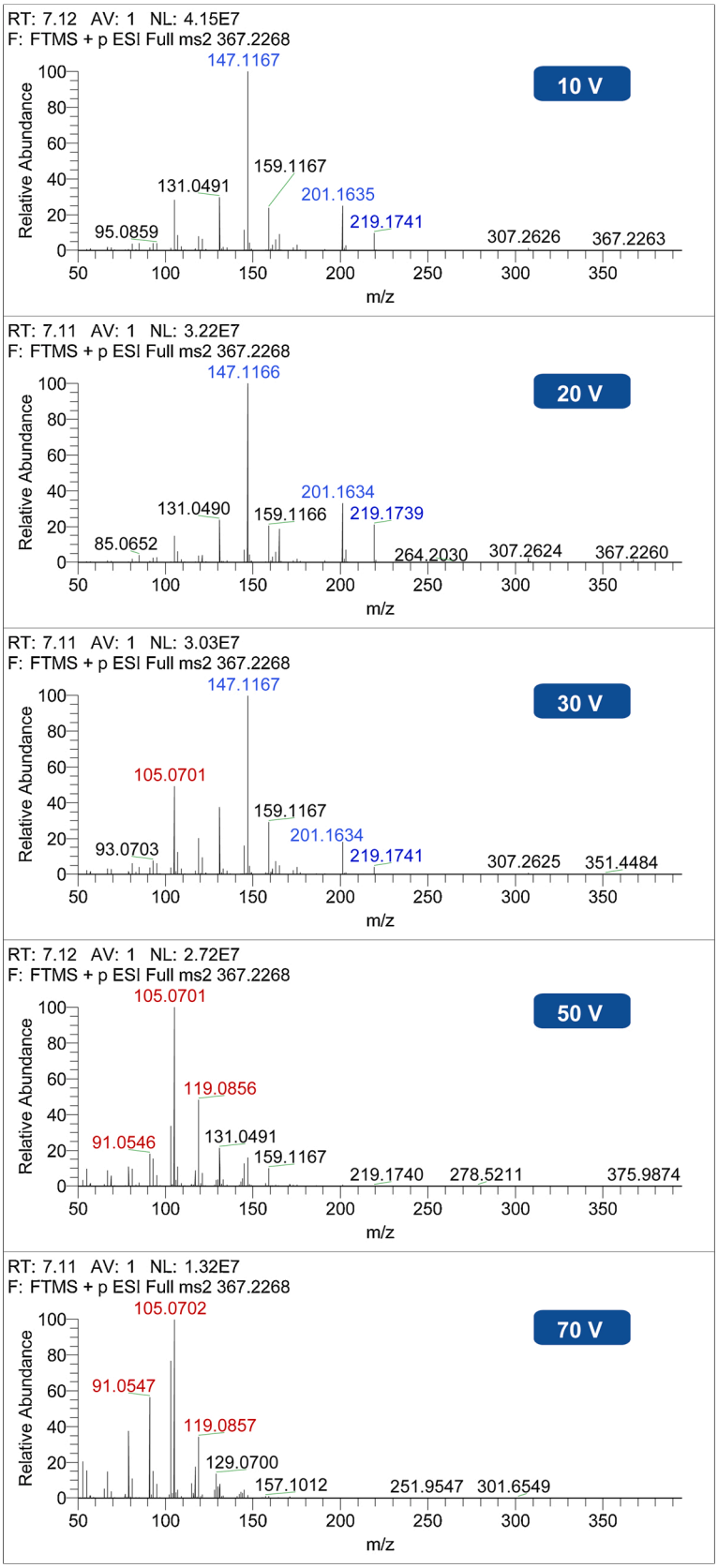

Fig. 13. Full MS scan and spectra of the peak with retention time 7.11 min corresponding to guayulin C at five different voltages (10, 20, 30, 50 and 70 V) in positive-ion mode.

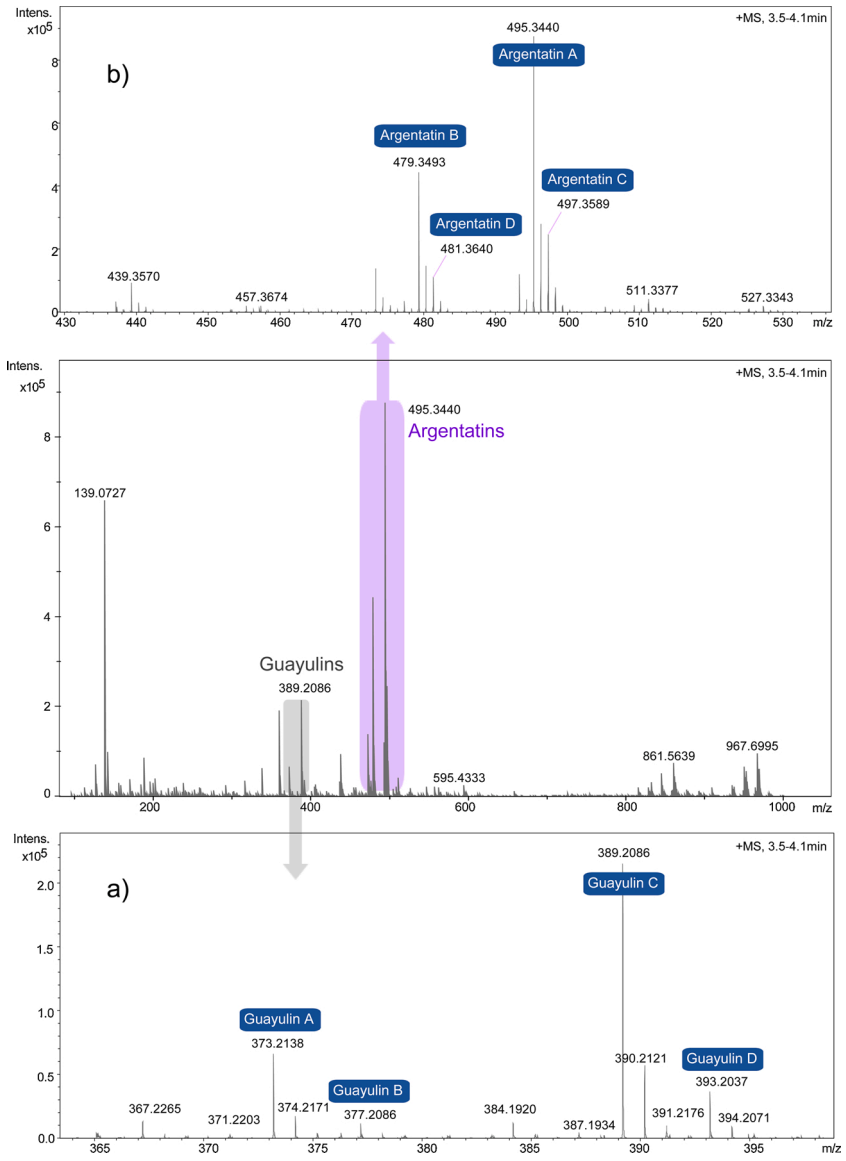

Fig. 14. Full ESI-MS scan of guayule resin. Amplification of regions corresponding to guayulins and argentatins.

FT-ICR-MS) with LC–MS would establish whether it is possible to use them to quantify guayulins from raw samples and, if so, to validate the methodology appropriately. Our results show that MALDI-TOF, in which chromatography is not used as a sample preparation step, can be very useful for monitoring the purification of guayulins; in particular, in monitoring the elimination of LMWNR that coexists in many resin extraction processes.

Finally, our findings show that the seasonal variation in the content of guayulins, especially guayulins A and B, which other authors have also observed, might be related to the biosynthesis of natural rubber that accelerates during the onset of winter. We are not aware that this possibility has been previously suggested, but it must also be corroborated by further studies.

CRediT authorship contribution statement

Juana Rozalén: Investigation. **M. Mercedes García:** Investigation. **Amaya Zalacain:** Investigation, Formal analysis, Visualization. **Horacio López-Córcoles:** Methodology, Investigation. **Jorge Hurtado de Mendoza:** Investigation. **Katrina Cornish:** Supervision, Writing - review & editing. **Manuel Carmona:** Conceptualization, Methodology, Validation, Visualization, Writing - review & editing, Project administration.

Declaration of Competing Interest

None declared.

Acknowledgements

This work was supported by the Spanish Ministry of Science and Innovation through the Ramón y Cajal Fellowships [RyC-2014-16307] and the GUARD Retos Project [RTI2018-098042-B100]. The authors wish to thank Agroservicios Guayule S.L. and Nokian Tyres Plc. for their support in this research, and to Dr. Kenneth McCreath for proof reading the manuscript.

References

Abdel-Haleem, H., Luo, Z., Ray, D., 2019. Genetic improvement of guayule (Parthenium argentatum A. Gray): an alternative rubber crop. In: Al-Khayri, J.M., Jain, S.M., Johnson, D.V. (Eds.), Advances in Plant Breeding Strategies: Industrial and Food Crops, 6. Springer, Cham, pp. 151–6178. https://doi.org/10.1007/978-3-030-23265-8_6.

Arreguin, B., Bonner, J., Wood, B.J., 1951. Studies on the mechanism of rubber formation in the guayule. III. Experiments with isotopic carbon. Arch. Biochem. Biophys. 31 (2), 234–247. https://doi.org/10.1016/0003-9861(51)90210-X.

Asakawa, Y., Noma, Y., 2010. Biotransformation of sesquiterpenoids. Comprehensive Natural Products II, pp. 803–892. https://doi.org/10.1016/b978-008045382-8.00066-6.

Bajwa, D.S., Holt, G.A., Bajwa, S.G., Duke, S.E., McIntyre, G., 2017. Enhancement of termite (Reticulitermes flavipes L.) resistance in mycelium reinforced biofiber-composites. Ind. Crops Prod. 107, 420–426. https://doi.org/10.1016/j.indcrop.2017.06.032.

Behl, H.M., Marchand, B., Rodríguez, E., 1983. Inheritance of sesquiterpenoid phenolic acid esters (Guayulins) in F1 hybrids of Parthenium (Asteraceae). Z. Naturforsch. C 38 (5-6), 494–496. https://doi.org/10.1515/znc-1983-5-631.

Benedict, C.R., Rosenfield, C.L., Ji, W., Foster, M.A., 2014. The low temperature induced rate of 3-hydroxy-3-methylglutaryl-CoA reductase in Parthenium argentatum Gray limits the theoretical rate of rubber formation. Ind. Crops Prod. 61, 176–179. https://doi.org/10.1016/j.indcrop.2014.06.054.

Bhatia, V.K., Masohan, A., 1983. Guayule (*Parthenium argentatum* A. Gray): an alternative to Hevea (Hevea brasiliensis). J. Sci. Ind. Res. 42, 273–280.

Bultman, J.D., Gilbertson, R.L., Adaskaveg, J., Amburgey, T.L., Parikh, S.V., Bailey, C.A., 1991. The efficacy of guayule resin as a pesticide. Bioresour. Technol. 35, 197–201. https://doi.org/10.1016/0960-8524(91)90030-N.

Chaves, M.H., Lago, J.H.G., Roque, N.F., 2003. Macrocarpane, a new sesquiterpene skeleton from the leaves of Porcelia macrocarpa. J. Braz. Chem. Soc. 14 (1) https://doi.org/10.1590/s0103-50532003000100004.

Cheng, F., Dehghanizadeh, M., Audu, M.A., Jarvis, J.M., Holguin, F.O., Brewer, C.E., 2020. Characterization and evaluation of guayule processing residues as potential feedstock for biofuel and chemical production. Ind. Crops Prod. 150, 112311 https://doi.org/10.1016/j.indcrop.2020.112311.

Chiang, C.C.K., Barkakaty, B., Puskas, J.E., Xie, W., Cornish, K., Peruch, F., Deffieux, A., 2014. Unraveling the mystery of natural rubber biosynthesis. Part II: composition and growth of in vitro natural rubber using high-resolution size exclusion chromatography. Rubber Chem. Technol. 87 (3), 451–458. https://doi.org/10.5254/rct.14.87913.

Coffelt, T.A., Ray, D.T., Dierig, D.A., 2015. 100 years of breeding guayule. In: Cruz, V.M., Dierig, A.E. (Eds.), Industrial Crops: Breeding for Bioenergy and Bioproducts. Springer, pp. 351–367. https://doi.org/10.1007/978-1-4939-1447-0_16.

Cornish, K., Scott, D.J., 2005. Biochemical regulation of rubber biosynthesis in guayule (Parthenium argentatum Gray). Ind. Crops Prod. 22, 49–58. https://doi.org/10.1016/j.indcrop.2004.04.032.

Cornish, K., Castillón, J., Scott, D.J., 2000. Rubber molecular weight regulation, in vitro, in plant species that produce high and low molecular weights in vivo. Biomacromolecules 1, 632–641. https://doi.org/10.1021/bm000034z.

Cornish, K., Williams, J.L., Kirk, M., Teetor, V.H., Ray, D.T., 2009. Evaluation & control of potential sensitizing & irritating chemical components in natural rubber latex extracted from the industrial crop guayule. Ind. Biotechnol. 5 (4), 245–252. https://doi.org/10.1089/ind.2009.5.245.

Cornish, K., Slutzky, J.L., Dasan, A.K.B., Kamenik, R.S., 2012. Biological and physical properties and performance of latices from different botanical sources, and effectiveness of some biobased fibers and fillers. In: Proceedings of the Latex and Synthetic Dispersions Conference, Paper 2. RAPRA, Kuala Lumpur, Malaysia, March 13-14, 2012.

Crevoisier, M., Steudle, K.C., Burgi, H.B., 1984. 3,3,1 l-Trimethyl-7-methylenetricyclo [6.3.0.02,4]undecane-5,1 l-diol, C15H240. Acta Cryst. C 40, 979–980.

Dong, N., Ponciano, G., McMahan, C.M., Coffelt, T.A., Johnson, L., Creelman, R., Whalen, M.C., Cornish, K., 2013. Overexpression of 3-hydroxy-3-ethylglutaryl coenzyme A reductase in Parthenium argentatum (guayule). Ind. Crops Prod. 46, 15–24.

Durán-Peña, M.J., Botubol, Ares J.M., Hanson, J.R., Collado, I.G., Hernández-Galán, R., 2015. Biological activity of natural sesquiterpenoids containing a gem-dimethylcyclopropane unit. Nat. Prod. Rep. 32 (8), 1236–1248. https://doi.org/10.1039/c5np00024f.

Foster, M.A., Coffelt, T.A., 2005. Guayule agronomics: establishment, irrigated production, and weed control. Ind. Crops Prod. 22 (1), 27–40. https://doi.org/10.1016/j.indcrop.2004.06.006.

Gijsen, H.J.M., Wijnberg, J.B.P.A., De Groot, A., 1995. Structure, occurrence, biosynthesis, biological activity, synthesis, and chemistry of aromadendrane sesquiterpenoids. In: Herz, W., Kirby, G.W., Moore, R.E., Steglich, W., Tamm, C. (Eds.), Progress in the Chemistry of Organic Natural Products, 64. Springer, Vienna, pp. 149–193. https://doi.org/10.1007/978-3-7091-9337-2_3.

Gilliland, M.G., Van Staden, J., 1986. Cyclic patterns of growth and rubber deposition in guayule Parthenium argentatum. Suggestions for a management programme. S. Afr. J. Plant Soil 3 (1), 21–26. https://doi.org/10.1080/02571862.1986.10634180.

Gilliland, M.G., van Staden, J., Bruton, A.G., 1984. Studies on the translocation system of guayule (*Parthenium argentatum* Gray). Protoplasma 122 (3), 169–177. https://doi.org/10.1007/BF01281694.

Guzman, J.D., 2014. Natural cinnamic acids, synthetic derivatives and hybrids with antimicrobial activity. Molecules 19 (12), 9292–19349. https://doi.org/10.3390/molecules191219292.

Hemida, A., Abdelrahman, M., 2020. Monitoring separation tendency of partial asphalt replacement by crumb rubber modifier and guayule resin. Constr. Build. Mater. 251, 118967 https://doi.org/10.1016/j.conbuildmat.2020.118967.

Holt, G.A., Chow, P., Wanjura, J.D., Pelletier, M.G., Coffelt, T.A., Nakayama, F.S., 2012. Termite resistance of biobased composition boards made from cotton byproducts and guayule bagasse. Ind. Crops Prod. 36 (1), 508–512. https://doi.org/10.1016/j.indcrop.2011.10.005.

Hou, T.-Y., Chiang-Ni, C., Teng, S.-H., 2019. Current status of MALDI-TOF mass spectrometry in clinical microbiology. J. Food Drug Anal. 27 (2), 404–414. https://doi.org/10.1016/j.jfda.2019.01.001.

Hunsaker, D.J., Elshikha, D.M., 2017. Surface irrigation management for guayule rubber production in the US desert Southwest. Agric. Water Manag. 185, 43–57. https://doi.org/10.1016/j.agwat.2017.01.015.

Hunsaker, D.J., Elshikha, D.M., Bronson, K.F., 2019. High guayule rubber production with subsurface drip irrigation in the US desert Southwestz. Agric. Water Manag. 220, 1–12. https://doi.org/10.1016/j.agwat.2019.04.016.

Ilut, D.C., Sanchez, P.L., Coffelt, T.A., Dyer, J.M., Jenks, M.A., Gore, M.A., 2017. A century of guayule: comprehensive genetic characterization of the US national guayule (*Parthenium argentatum* A. Gray) germplasm collection. Ind. Crops Prod. 109, 300–309. https://doi.org/10.1016/j.indcrop.2017.08.029.

Jara, F.M., Cornish, K., Carmona, M., 2019. Potential applications of guayulins to improve feasibility of guayule cultivation. Agronomy 9 (12), 804. https://doi.org/10.3390/agronomy9120804.

Ji, Wan, Benedict, C.R., Foster, M.A., 1993. Seasonal variations in rubber biosynthesis, 3-hydroxy-3-methylglutaryl-coenzyme A reductase, and rubber transferase activities in Parthenium argentatum in the Chihuahuan Desert. Plant Physiol. 103 (2), 535–542.

Kajiura, H., Suzuki, N., Mouri, H., Watanabe, N., Nakazawa, Y., 2018. Elucidation of rubber biosynthesis and accumulation in the rubber producing shrub, guayule (Parthenium argentatum Gray). Planta 247 (2), 513–526. https://doi.org/10.1007/s00425-017-2804-7.

Luo, Z., Abdel-Haleem, H., 2019. Phenotypic diversity of USDA guayule germplasm collection grown under different irrigation conditions. Ind. Crops Prod. 142, 111867 https://doi.org/10.1016/j.indcrop.2019.111867.

Lusher, S.M., Richardson, D.N., 2015. Guayule plant extracts as recycling agents in hot mix asphalt with high reclaimed binder content. J. Mater. Civil Eng. 27 (10), 04014269 https://doi.org/10.1061/(ASCE)MT.1943-5533.0001238.

Maatooq, G.T., 2002. Microbial metabolism of partheniol by Mucor circinelloides. Phytochem. 59 (1), 39–44. https://doi.org/10.1016/S0031-9422(01)00412-5.

Maatooq, G.T., 2003. Microbiological and chemical transformations of argentatin B. Z. Naturforschung C. 58 (3-4), 249–255. https://doi.org/10.1515/znc-2003-3-419.

Maatooq, G.T., Stumpf, D.K., Hoffmann, J.J., Hutter, L.K., Timmermann, B.N., 1996. Antifungal eudesmanoids from Parthenium argentatum x P. tomentosa. Phytochem 41 (2), 519–524. https://doi.org/10.1016/0031-9422(95)00580-3.

Martínez, M., Flores, G., Romo de Vivar, A., Reynolds, G., Rodríguez, E., 1986. Guayulins C and d from guayule (Parthenium argentatum). J. Nat. Prod. 49, 1102–1103. https://doi.org/10.1021/np50048a022.

Mears, J.A., Larson, R.A., 1982. Rubber and allergenic terpenes: possible problems in guayule commercialization. J. Arid Environ. 5 (2), 169–178. https://doi.org/10.1016/S0140-1963(18)31547-7.

Nakayama, F.S., 2005. Guayule future development. Ind. Crops Prod. 22 (1), 3–13. https://doi.org/10.1016/j.indcrop.2004.05.006.

Nakayama, F.S., Vinyard, S.H., Chow, P., Bajwa, D.S., Youngquist, J.A., Muehl, J.H., Krzysik, A.M., 2001. Guayule as a wood preservative. Ind. Crops Prod. 14 (2), 105–111. https://doi.org/10.1016/s0926-6690(00)00093-5.

Pascual-Villalobos, M.J., López, M.D., 2013. New application of guayule resin in controlled release formulations. Ind. Crops Prod. 43 (1), 44–49. https://doi.org/10.1016/j.indcrop.2012.07.001.

Payne, M.E., Grayson, S.M., 2018. Characterization of synthetic polymers via matrix assisted laser desorption ionization time of flight (MALDI-TOF) mass spectrometry. J. Vis. Exp. 136, e57174 https://doi.org/10.3791/57174.

Pearson, C.H., Cornish, K., Rath, D.J., 2013. Extraction of natural rubber and resin from guayule using an accelerated solvent extractor. Ind. Crops Prod. 43 (1), 506–510. https://doi.org/10.1016/j.indcrop.2012.06.052.

Placido, D.F., Dierig, D.A., Cruz, V.M.V., Ponciano, G., Dong, C., Dong, N., Huynh, T., Williams, T., Cahoon, R.E., Wall, G.W., Wood, D.F., McMahan, C., 2020. Downregulation of an allene oxide synthase gene improves photosynthetic rate and alters phytohormone homeostasis in field-grown guayule. Ind. Crops Prod. 153, 112341 https://doi.org/10.1016/j.indcrop.2020.112341. https://www.

Proksch, P., Mohan Behl, H., Rodríguez, E., 1981. Detection and quantification of guayulins A and B in Parthenium argentaturn (guayule) and F1 hybrids by high-performance liquid chromatography. J. Chromatogr. A 213 (2), 345–348. https://doi.org/10.1016/S0021-9673(00)81920-2.

Ray, D.T., Veatch-Blohm, M.E., Teetor, V.H., Walsh, B., 2007. Upper and lower heritability estimates in guayule based on mode of reproduction. J. Am. Soc. Hortic. Sci. 132 (2), 213–218. https://doi.org/10.21273/JASHS.132.2.213.

Romo de Vivar, A., Martínez-Vázquez, M., Matsubara, C., Pérez, G., Joseph-Nathan, P., 1990. Triterpenes in Parthenium argentatum. Phytochem 29, 915–918.

Schloman, W.W., Hively, R.A., Krishen, A., Andrews, A.M., 1983. Guayule byproduct evaluation: extract characterization. J. Agric. Food Chem. 31 (4), 873–876. https://doi.org/10.1021/jf00118a050.

Schloman, W.W., Garrot, D.J., Ray, D.T., Bennett, D.J., 1986. Seasonal effects on guayule resin composition. J. Agric. Food Chem. 34 (2), 177–179. https://doi.org/10.1021/jf00068a005.

Schloman, W.W., Hilton, A.S., McGrady, J.J., 1991. Allelopathic response of vegetables to guayule residue. Bioresour. Technol. 35 (2), 191–196. https://doi.org/10.1016/0960-8524(91)90029-j.

Sfeir, N., Chapuset, T., Palu, S., Lançon, F., Amor, A., García García, J., Snoeck, D., 2014. Technical and economic feasibility of a guayule commodity chain in Mediterranean Europe. Ind. Crops Prod. 59, 55–62. https://doi.org/10.1016/j.indcrop.2014.04.043.

Sidhu, O.P., Ratti, N., Behl, H.M., 1995. Quantitative and qualitative variations in resin content and guayulins (A and B) among different guayule cultivars. J. Agric. Food Chem. 43, 2012–2015 https://doi.org/10.1021/jf00056a010.

Snoeck, D., Chapuset, T., García García, J., Sfeir, N., Palu, S., 2015. Feasibility of a guayule commodity chain in the Mediterranean region. Ind. Crops Prod. 75, 159–164. https://doi.org/10.1016/j.indcrop.2015.05.008.

Soratana, K., Rasutis, D., Azarabadi, H., Eranki, P.L., Landis, A.E., 2017. Guayule as an alternative source of natural rubber: a comparative life cycle assessment with Hevea and synthetic rubber. J. Clean Prod. 159, 271–280. https://doi.org/10.1016/j.jclepro.2017.05.070.

Spano, N., Meloni, P., Idda, I., Mariani, A., Pilo, M., Nurchi, V., Lachowicz, J.I., Rivera, E., Orona-Espino, A., Sanna, G., 2018. Assessment, validation and application to real samples of an RP-HPLC method for the determination of guayulins a, B, C and d in Guayule Shrub. Separations 5, 23. https://doi.org/10.3390/separations5020023.

Suchat, S., Pioch, D., Palu, S., Tardan, E., van Loo, E.N., Davrieux, F., 2013. Fast determination of the resin and rubber content in Parthenium argentatum biomass using near infrared spectroscopy. Ind. Crops Prod. 45, 44–51. https://doi.org/10.1016/j.indcrop.2012.09.025.

Taurines, M., Brancheriau, L., Palu, S., Pioch, D., Tardan, E., Boutahar, N., Sartre, P., Meunier, F., 2019. Determination of natural rubber and resin content of guayule fresh biomass by near infrared spectroscopy. Ind. Crops Prod. 134, 177–184. https://doi.org/10.1016/j.indcrop.2019.03.073.

Teetor, V.H., Ray, D.T., Schloman, W.W., 2009. Evaluating chemical indices of guayule rubber content: guayulins A and B. Ind. Crops Prod. 2-3, 590–598. https://doi.org/10.1016/j.indcrop.2008.11.005.

Thompson, A.E., Ray, D.T., Livingston, M., Dierig, D.A., 1988. Variability of rubber and plant growth characteristics among single plant selections from a diverse guayule breeding population. J. Am. Soc. Hort. Sci. 113, 608–611.

Tran, D.N., Cramer, N., 2014. Biomimetic synthesis of (+)-Ledene, (+)-Viridiflorol, (−)-Palustrol, (+)-Spathulenol, and Psiguadial A, C, and D via the Platform Terpene (+)-Bicyclogermacrene. Chem. Eur. J. 20 (34), 10654–10660. https://doi.org/10.1002/chem.201403082.

Veatch, M.E., Ray, D.T., Mau, C.J.D., Cornish, K., 2005. Growth, rubber, and resin evaluation of two-year-old transgenic guayule. Ind. Crops Prod. 22 (1), 65–74. https://doi.org/10.1016/j.indcrop.2004.06.007.

Walter, E.D.J., 1944. Isolation of partheniol, parthenyl ciamate, and other constituents from guayule resin. Am. Chem. Soc. 66, 419.

Wu, T., Zhang, C., Ren, H., Xi, Y., Du, Y., Peng, Y., 2017. Solvent effect in polymer analysis by MALDI-TOF mass spectrometry. Int. J. Polym. Anal. Charact. 22 (2), 160–168. https://doi.org/10.1080/1023666X.2016.1263913.

Zoeller, J.H.J., Wagner, J.P., Sulikowski, G.A., 1994. Concise multigram purification of guayulin A from guayule. J. Agric. Food Chem. 42 (8), 1647–1649. https://doi.org/10.1021/jf00044a012.